SUPPORTING INFORMATION

Lanthanide-based luminescent probes for biological magnesium: accessing polyphosphate-bound Mg^{2+}

*Brismar Pinto-Pacheco, Qitian Lin, Claudia W. Yan, Symara de Melo Silva, and Daniela Buccella**

Department of Chemistry, New York University, New York, New York 10003

S1. Supporting Figures

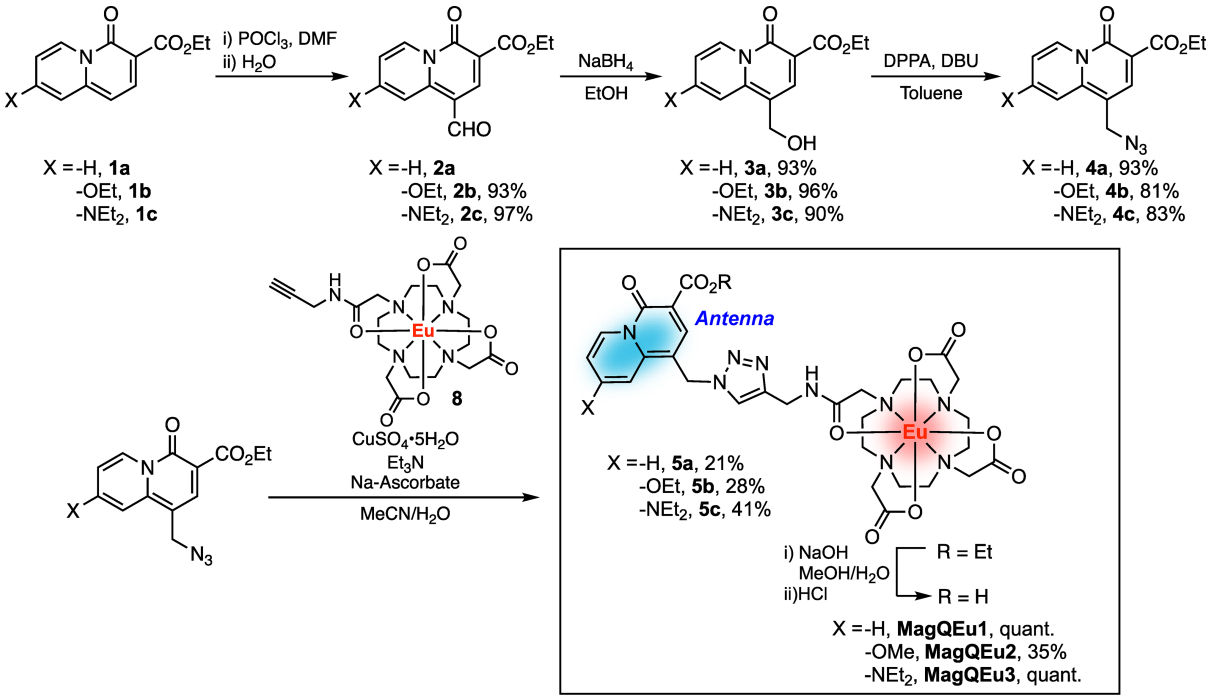

Scheme S1. Synthesis of **MaQEu1-3** family of sensors.

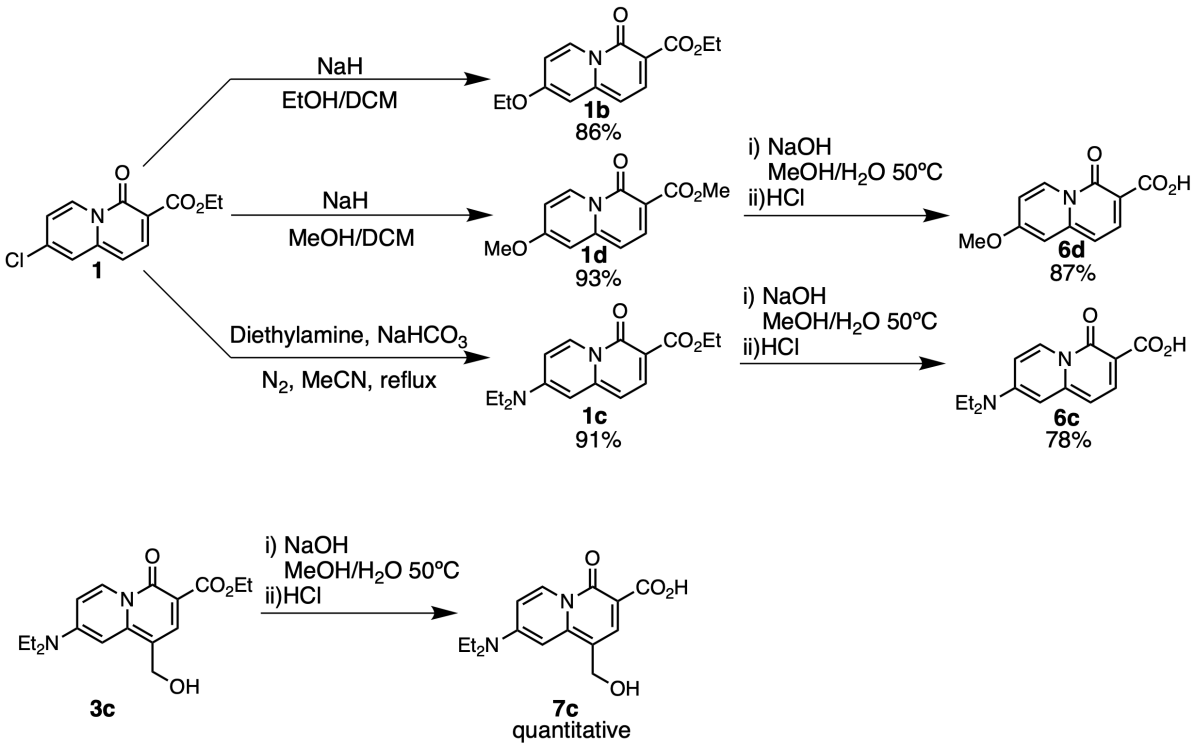

Scheme S2. Synthesis of antenna precursors.

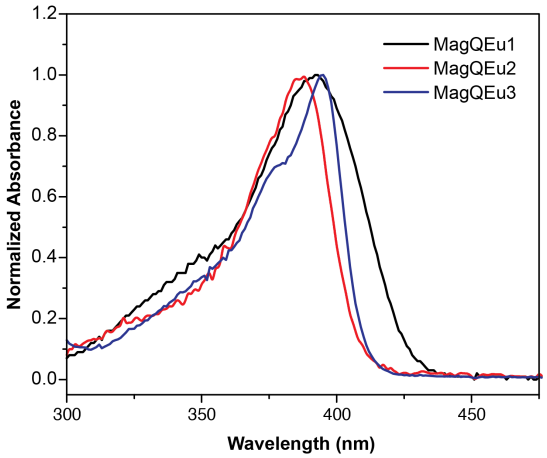

Figure S1. Absorption spectra of **MagQEu1**, **MagQEu2** and **MagQEu3** in aqueous buffer (50 mM PIPES, 100 mM KCl, pH 7.0) at 25 °C.

Table S1. Luminescence lifetime of **MagQEu1** in presence and absence of analytes.

Compound	τ_{H2O}[a] **(ms)**	τ_{D2O}[b] **(ms)**	q[c]
MagQEu1	0.220 ± 0.003	0.308 ± 0.010	1.1 ± 0.1
MagQEu1 + Mg^{2+}	0.505 ± 0.009	1.269 ± 0.053	1.02 ± 0.05
MagQEu1 +MgATP	0.468 ± 0.005	1.109 ± 0.060	1.06 ± 0.06

[a]Measured in 100 mM PIPES, 50 mM KCl, pH 7.0. [b]Measured in 100 mM PIPES, 50 mM KCl, buffer in D_2O, pD 7.12. [c]Calculated using Horrock's equation for Eu: $q = 1.11(\tau^{-1}_{H2O} - \tau^{-1}_{D2O} - 0.31)$, Ref.[1]

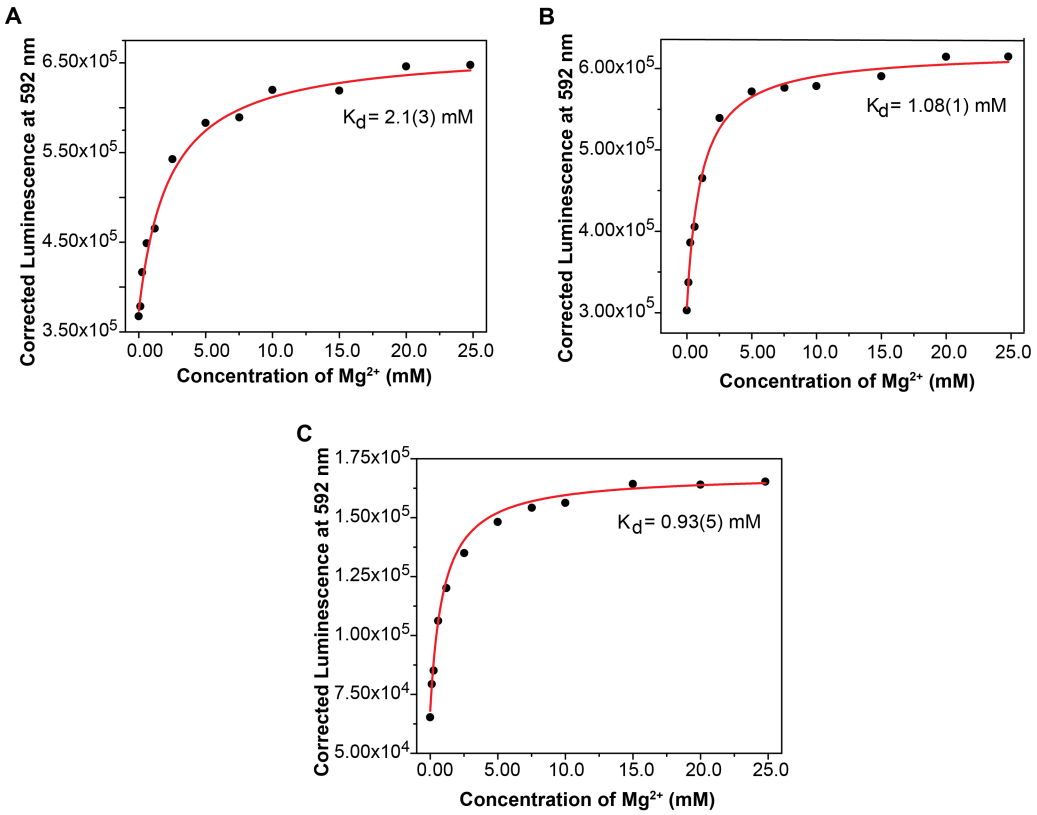

Figure S2. Representative non-linear fit of corrected luminescence at 592 nm of (A) **MagQEu1** (B) **MagQEu2** and (C) **MagQEu3** (5 μM) in response to increasing concentrations of Mg^{2+} (50 mM PIPES, 100 mM KCl, pH 7.0) at 25 °C. K_d values represent the average of three titrations; numbers in parenthesis correspond to uncertainty in the last significant figure. Delayed detection: 0.1 ms.

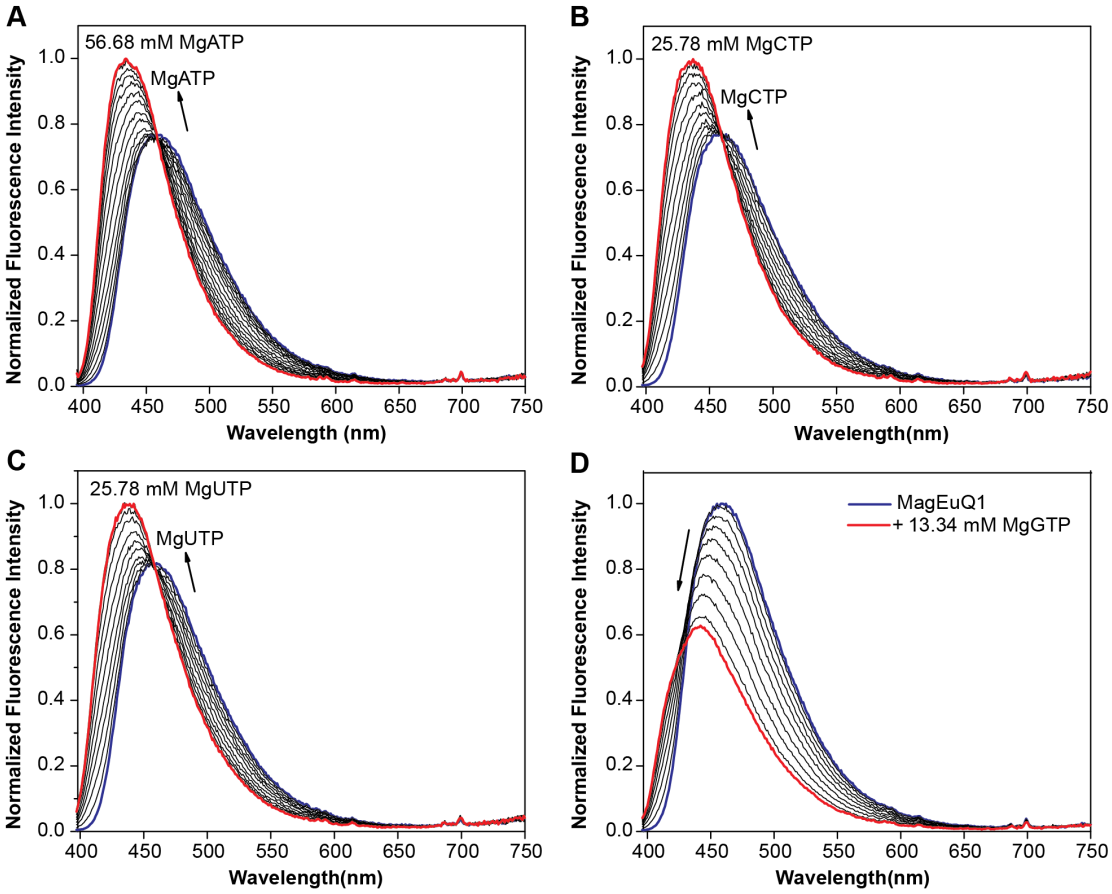

Figure S3. Steady-state luminescence spectra of **MagQEu1** (5 µM) in response to increasing concentrations of MgATP (A), MgCTP (B), MgUTP (C) or MgGTP (D) in aqueous buffer (50 mM PIPES, 100 mM KCl, pH 7.0) at 25 °C.

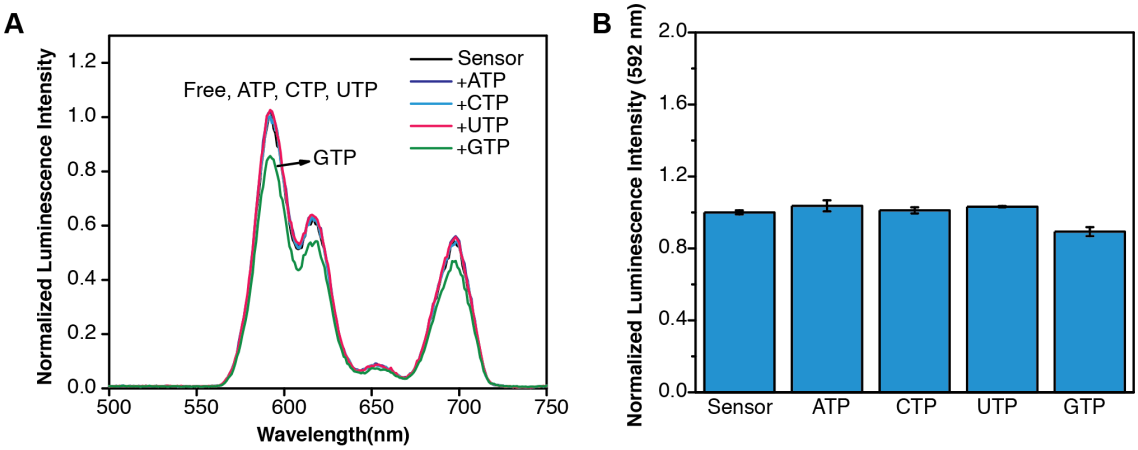

Figure S4. (A) Time-resolved luminescence spectra of **MagQEu1** (5 µM) upon treatment with various nucleoside triphosphates (5 mM) in aqueous buffer (50 mM PIPES, 100 mM KCl, pH 7.0) at 25 °C. Delayed detection: 0.1 ms. (B) Luminescence intensity at 592 nm. Averages of triplicate measurements.

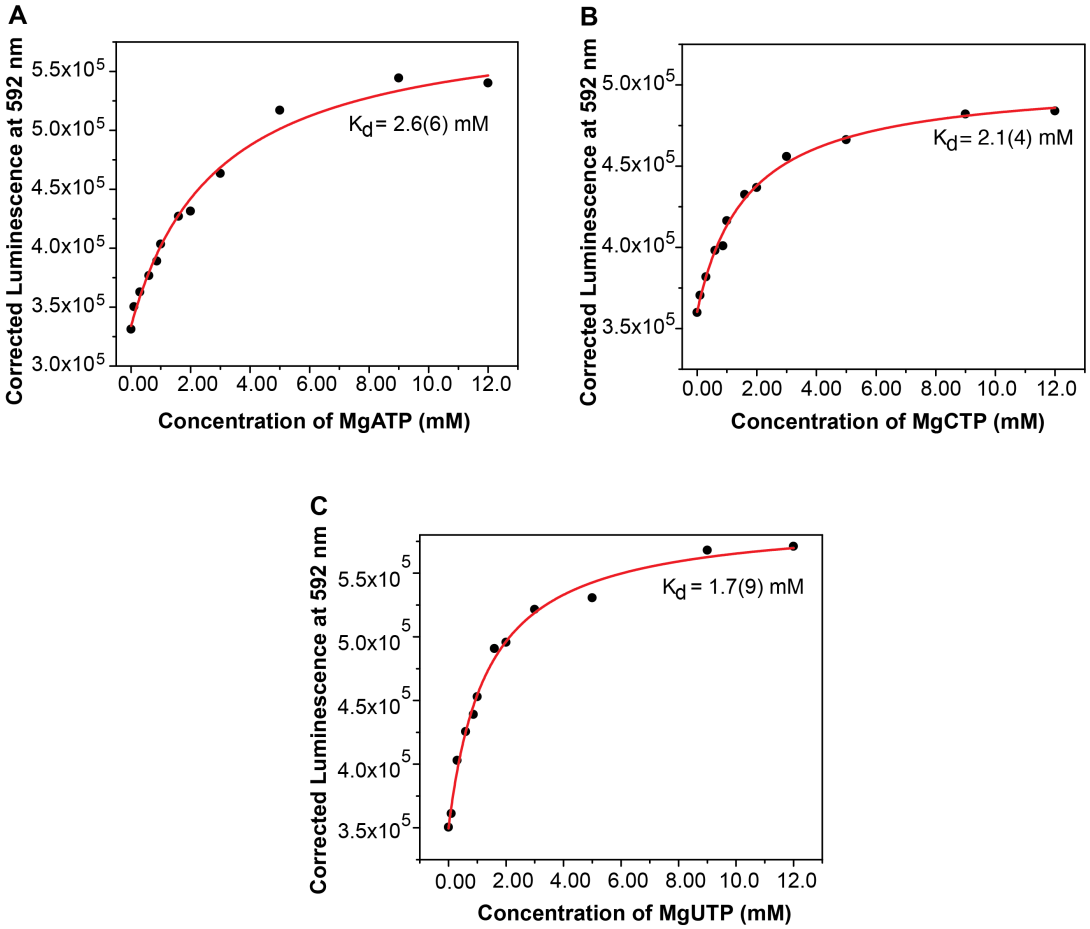

Figure S5. Non-linear fit of corrected luminescence at 592 nm of **MagQEu1** (5 μM) in response to increasing concentrations of MgATP (A) MgCTP (B), or MgUTP (C) in aqueous buffer (50 mM PIPES, 100 mM KCl, pH 7.0) at 25 °C. K_d values represent the average of three titrations; numbers in parenthesis correspond to uncertainty in the last significant figure. Delayed detection: 0.1 ms.

Table S2. Electrochemical properties of various antennas in acetonitrile.

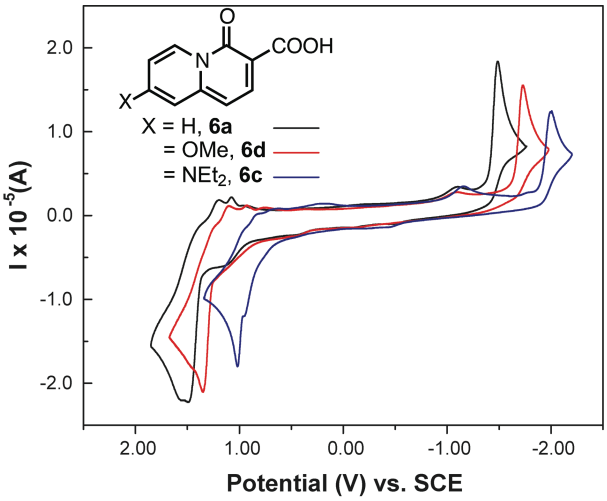

Chelator	Ep (A/A-)/ V vs. SCE[a]	E00/eV[b]
6a	-1.49	2.91
6d	-1.75	3.00
6c	-2.00	3.03

[a]All redox potentials measured in acetonitrile containing 0.1 M Bu_4NPF_6. [b]Calculated as the midpoint between the absorption and emission maxima in the acetonitrile.

Table S3. Driving force for PeT (ΔG_{PeT}) from the various nucleobases to the antennas **6a, 6c** and **6d** in acetonitrile.

Nucleobase	ΔG_{PeT}/eV for antenna 6a	ΔG_{PeT}/eV for antenna 6d	ΔG_{PeT}/eV for antenna 6c
Guanine	-0.17	0.00	0.22
Adenine	0.30	0.47	0.69
Cytosine	0.48	0.65	0.87
Uracil	0.73	0.90	1.12

ΔG_{PeT} were estimated from redox potentials in acetonitrile using the Rehm-Weller equation $\Delta G_{PeT} = E(D^+/D) - E(A/A^-) - E_{00} - w_p$, wih $E(D^+/D)$, $E(A/A^-)$, E_{00} and w_p represent the oxidation potential (written as a reduction) of the electron donor, reduction potential of the electron acceptor, the excitation energy of the quinolizine, and the electrostatic work term, respectively. The electrostatic work term can be neglected due to the high dielectric constant of acetonitrile. The nucleobases were used as donors and the antennas as acceptors. The oxidation potentials of the nucleobases were obtained from Ref. [2].

Note: Cyclic and linear sweep voltammetry were also conducted to estimate the effect of Mg^{2+} coordination on the reduction potential of the antenna. Addition of increasing amounts of $Mg(ClO_4)_2$ led to a progressive broadening and shift in the cathodic peak, with as much as +80 mV shift in the presence of five equivalents of the metal. This behavior was expected, as the coordination of Mg^{2+} withdraws electron density from the chelator and facilitates the reduction. Thus, PeT in the presence of MgGTP becomes even more thermodynamically favorable for the unsubstituted quinolizine 6a, and it may become favorable for 6d. This anodic shift, however, does not seem large enough to make the photoreduction of chelator 6c favorable.

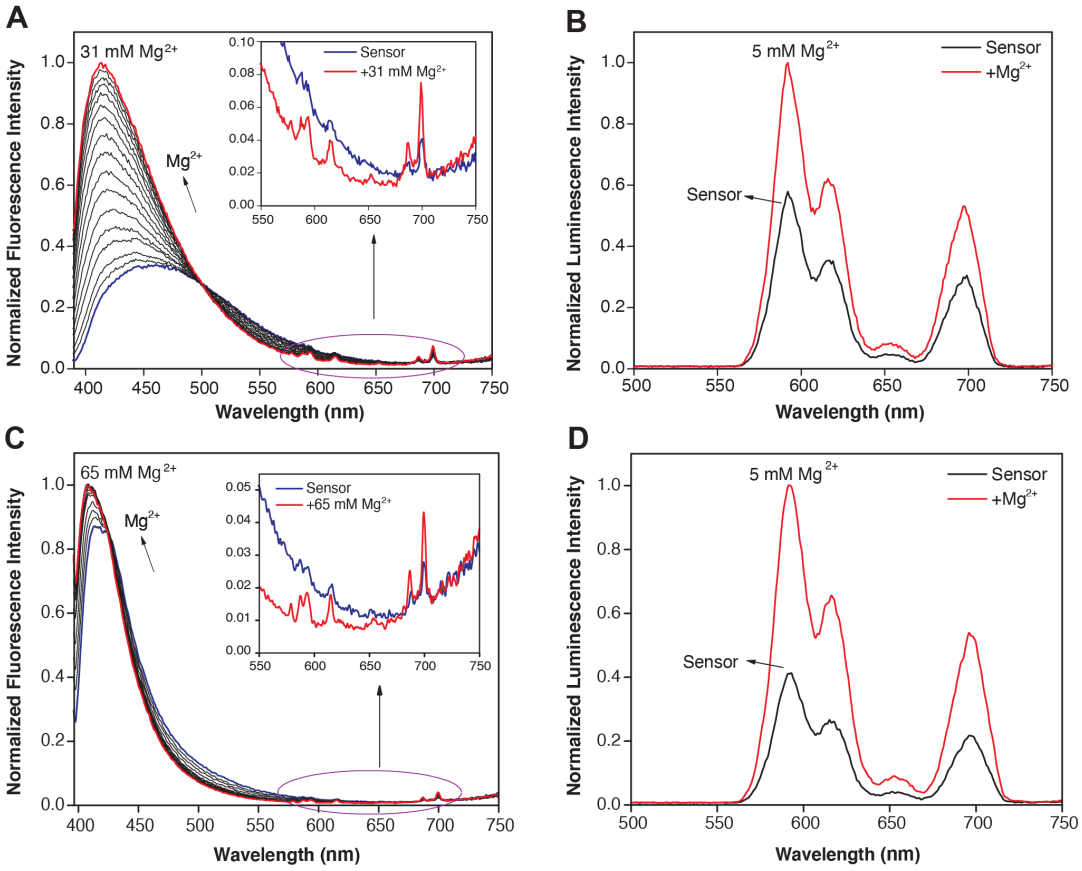

Figure S6. Steady-state (A, C) and time gated (B, D) luminescence spectra of **MagQEu2** (A, B) and **MagQEu3** (C, D) in response to increasing concentrations of Mg^{2+} in aqueous buffer (50 mM PIPES, 100 mM KCl, pH 7.0) at 25 °C. Sensor concentration= 5 µM. Delayed detection: 0.1 ms.

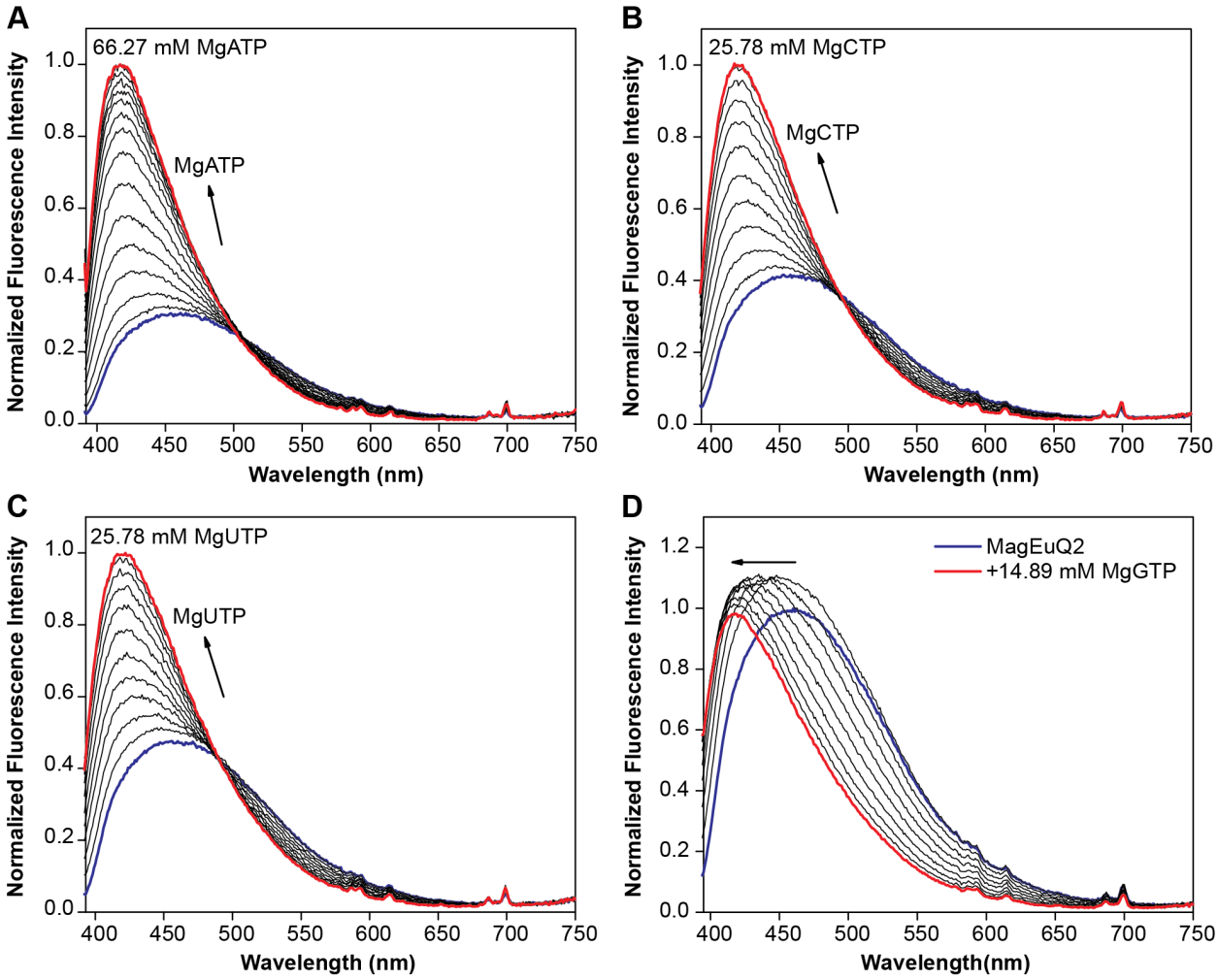

Figure S7. Steady-state luminescence spectra of **MagQEu2** (5 μM) in response to increasing concentrations of MgATP (A), MgCTP (B), MgUTP (C) or MgGTP (D) in aqueous buffer (50 mM PIPES, 100 mM KCl, pH 7.0) at 25 °C.

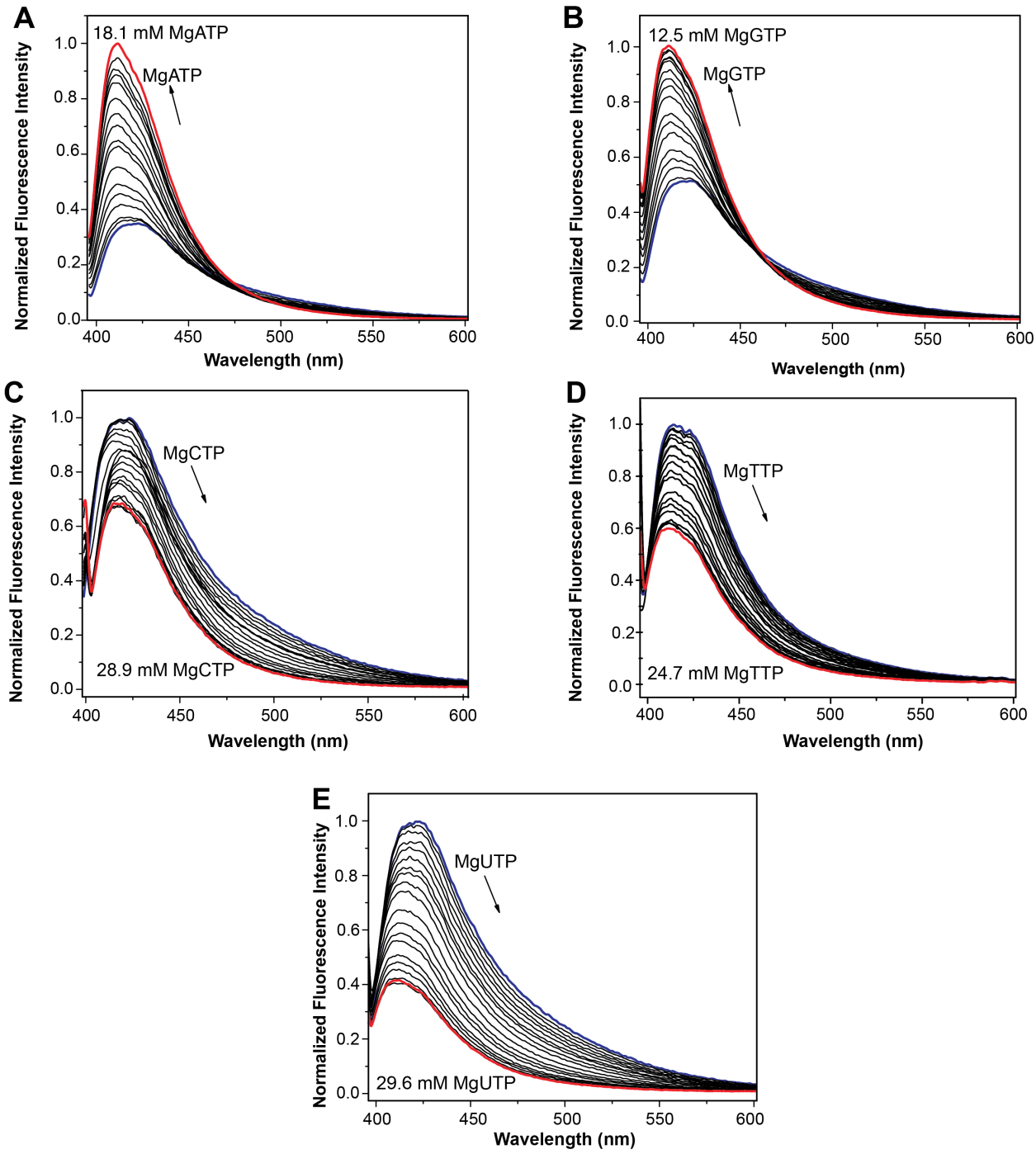

Figure S8. Steady-state luminescence spectra of **MagQEu3** (5 μM) in response to increasing concentrations of MgATP (A), MgGTP (B), MgCTP (C), MgTTP (D) or MgUTP (E) in aqueous buffer (50 mM PIPES, 100 mM KCl, pH 7.0) at 25 °C.

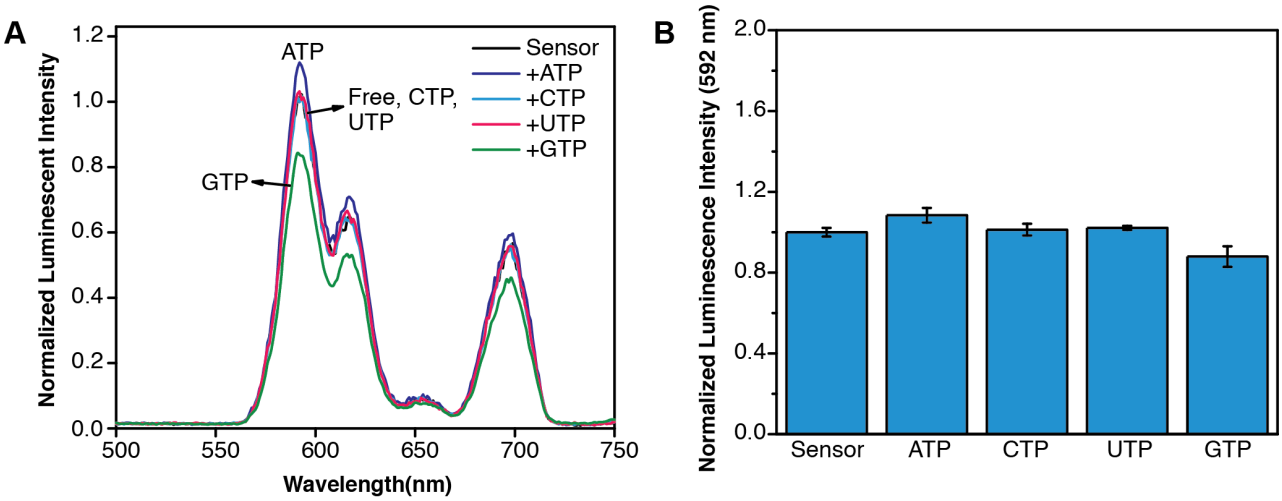

Figure S9. (A) Time-resolved luminescence spectra of **MagQEu2** (5 μM) upon treatment of various nucleoside triphosphates (5 mM) in aqueous buffer (50 mM PIPES, 100 mM KCl, pH 7.0) at 25 °C. Delayed detection: 0.1 ms. (B) Luminescence intensity at 592 nm. Averages of triplicate measurements.

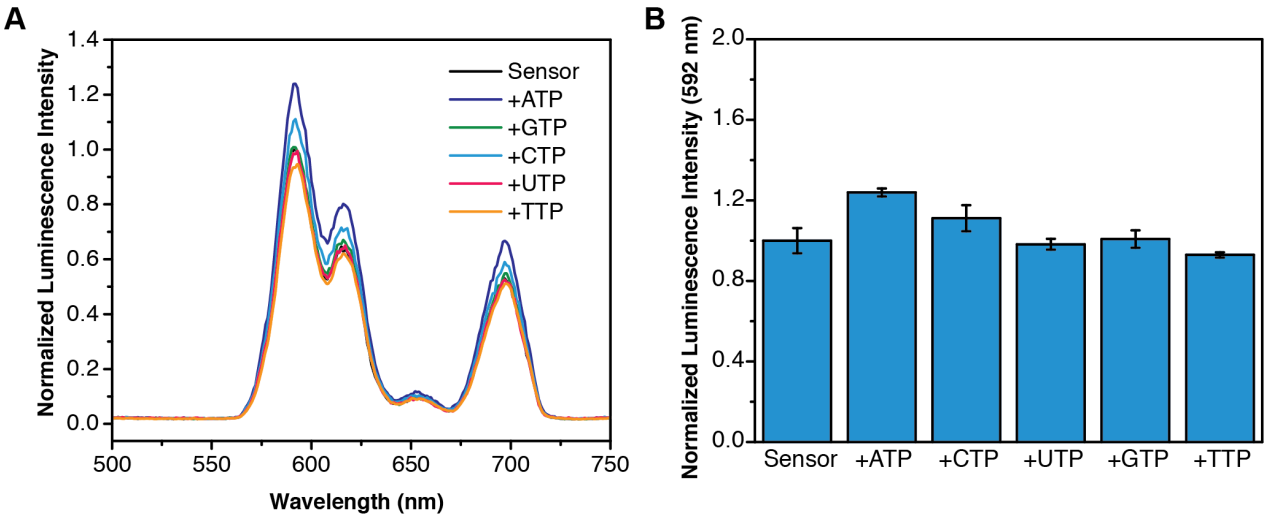

Figure S10. (A) Time-resolved luminescence spectra of **MagQEu3** (5 μM) upon treatment of various nucleoside triphosphates (5 mM) in aqueous buffer (50 mM PIPES, 100 mM KCl, pH 7.0) at 25 °C. Delayed detection: 0.1 ms. (B) Luminescence intensity at 592 nm. Averages of triplicate measurements.

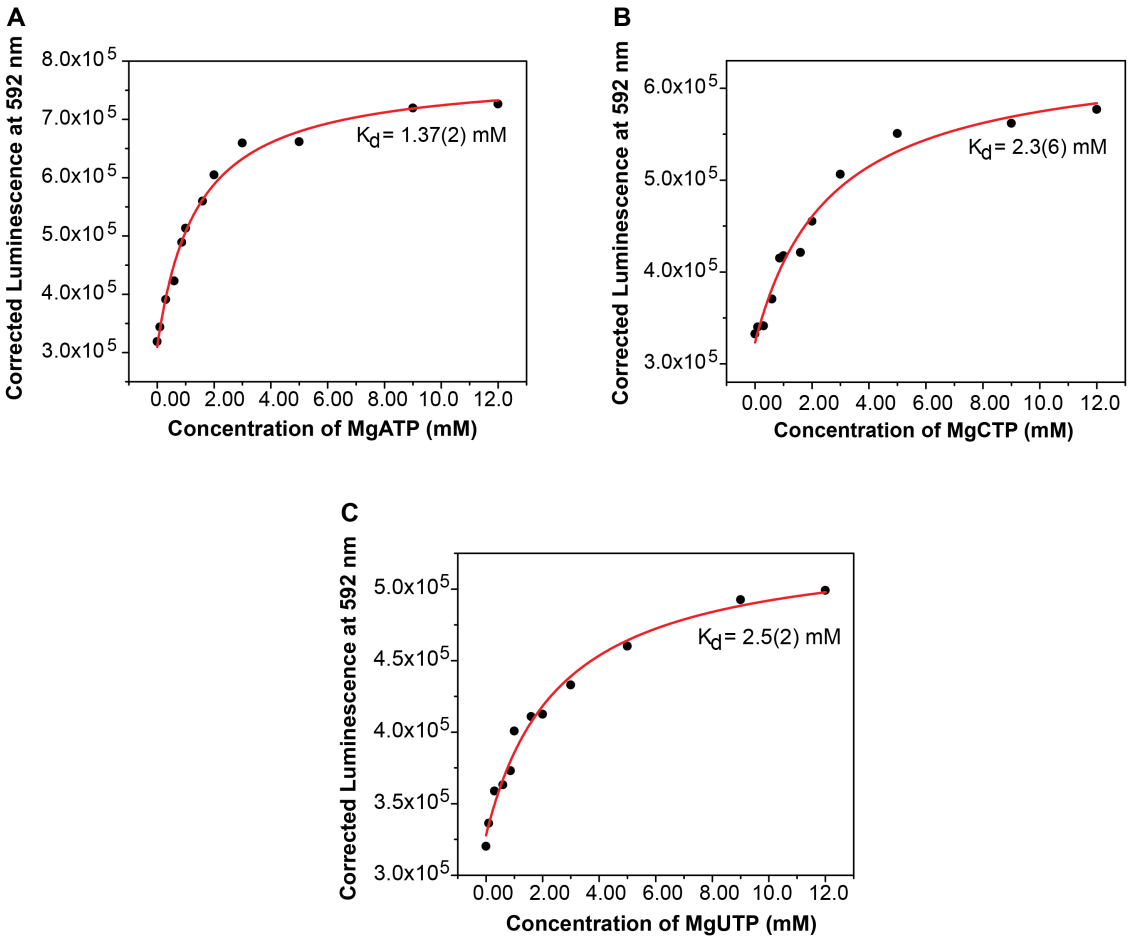

Figure S11. Non-linear fit of corrected luminescence at 592 nm of **MagQEu2** (5 μM) in response to increasing concentrations MgATP (A) and MgCTP (B) or MgUTP (C) aqueous buffer (50 mM PIPES, 100 mM KCl, pH 7.0) at 25 °C. Delayed detection: 0.1 ms.

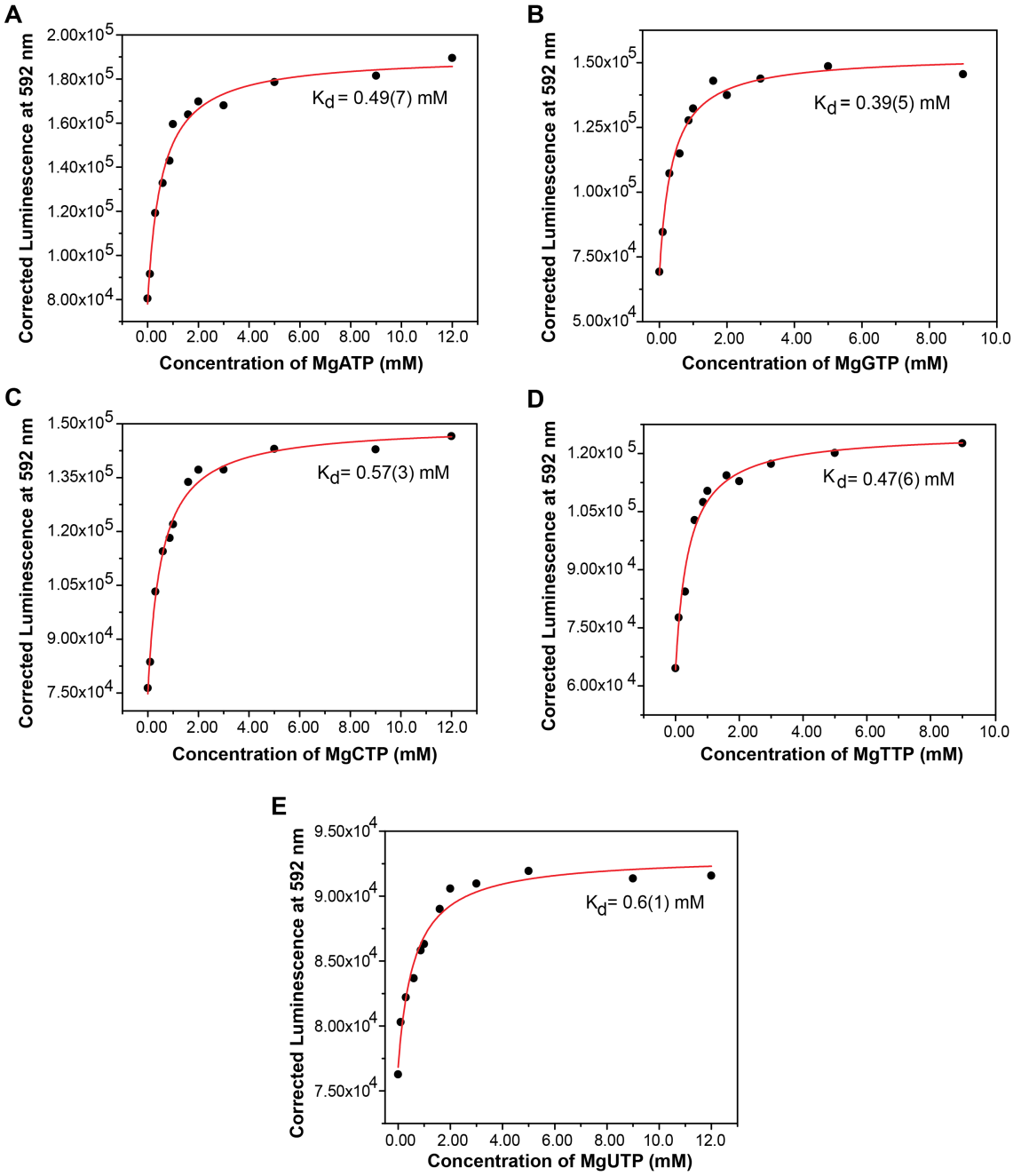

Figure S12. Non-linear fit of corrected luminescence at 592 nm of **MagQEu3** (5 μM) in response to increasing concentrations MgATP (A) and MgGTP (B) MgCTP (C), MgTTP (D) or MgUTP (E) aqueous buffer (50 mM PIPES, 100 mM KCl, pH 7.0) at 25 °C. Delayed detection: 0.1 ms.

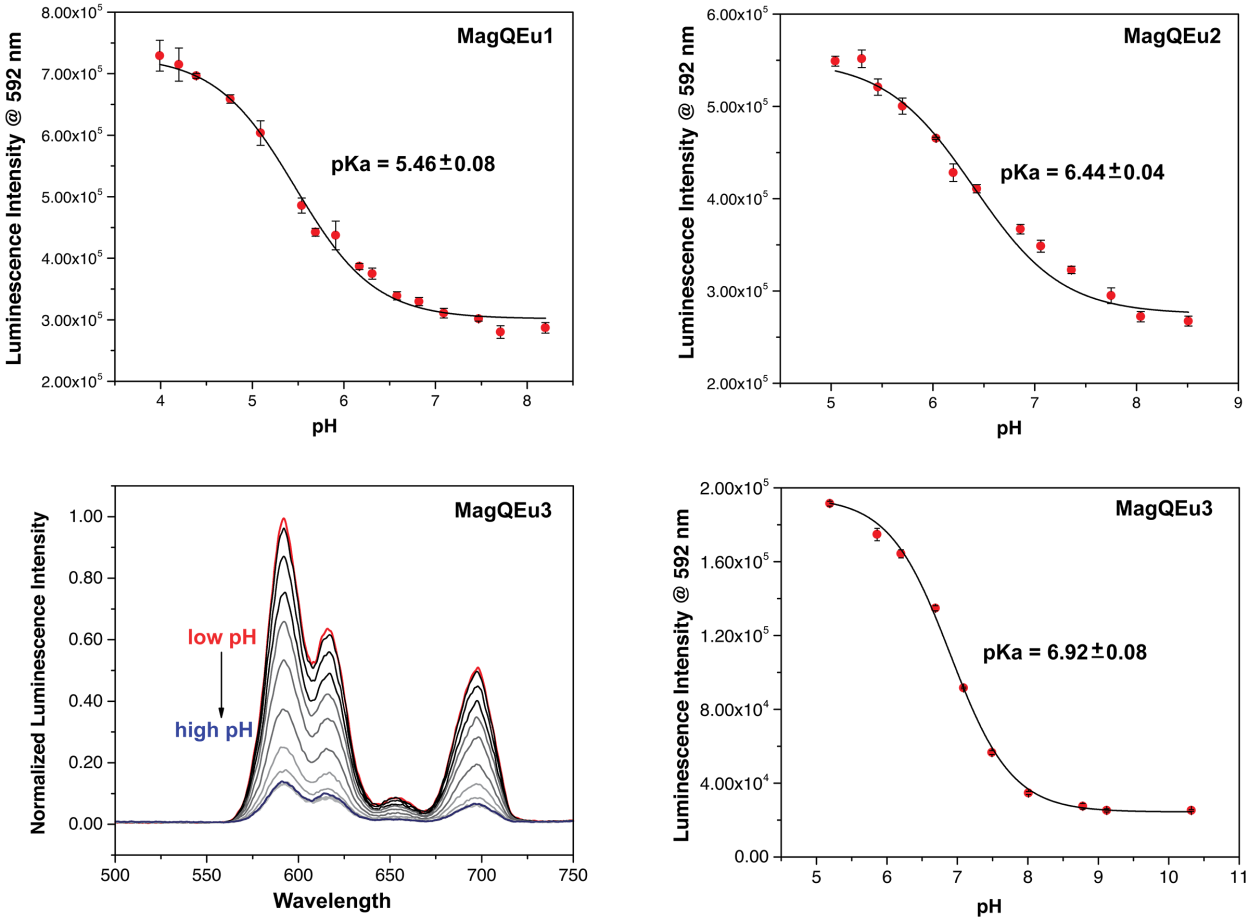

Figure S13. Determination of pKa of **MagQEu1-3.** Measurements conducted with 5 μM sensor in aqueous solution at 25 °C, exciting at the corresponding maximum of each antenna. Delayed detection: 0.1 ms.

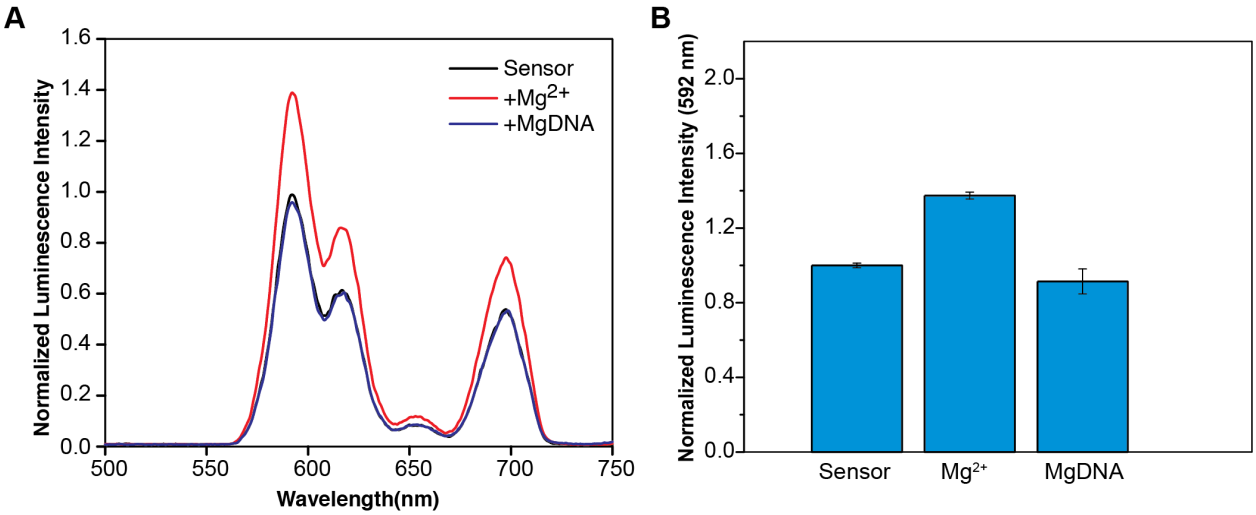

Figure S14. (A) Time-resolved luminescence spectra of **MagQEu1** (5 μM) upon treatment with DNA (2 mM [P]), free Mg^{2+} (1 mM) or MgDNA (1 mM in Mg, [Mg]/[P] = 0.5) in aqueous buffer (50 mM PIPES, 100 mM KCl, pH 7.0) at 25 °C. Delayed detection: 0.1 ms. (B) Luminescence intensity at 592 nm. Averages of triplicate measurements.

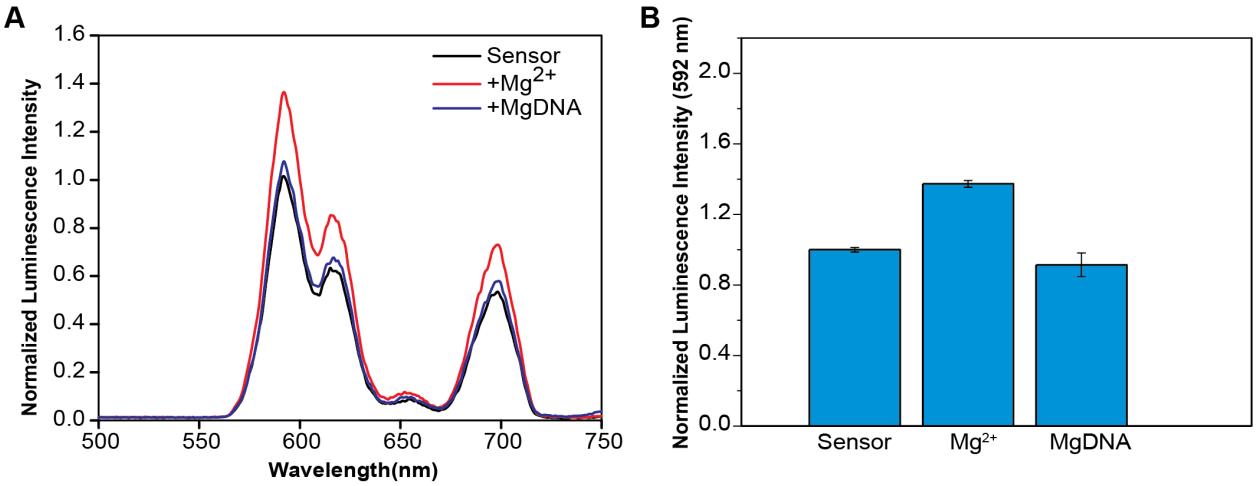

Figure S15. (A) Time-resolved luminescence spectra of **MagQEu2** (5 μM) upon treatment with DNA (2 mM [P]), free Mg^{2+} (1 mM) or MgDNA (1 mM in Mg, [Mg]/[P] = 0.5) in aqueous buffer (50 mM PIPES, 100 mM KCl, pH 7.0) at 25 °C. Delayed detection: 0.1 ms. (B) Luminescence intensity at 592 nm. Averages of triplicate measurements.

S2. Experimental procedures

S2.1 Synthetic Procedures

Compounds **1**[3]**, 1a**[3]**, 2a**[3], **6a**[3] and **8**[4] were synthesized according to reported procedures. All NMR spectra were acquired either on a Bruker Avance 400 NMR or Avance III-600 NMR spectrometer equipped with a 5 mm sample diameter Inverse Quadruple Resonance Probe. ^{1}H NMR chemical shifts are reported in ppm relative to $SiMe_4$ ($\delta = 0$) and were referenced internally with respect to residual protio impurity in the solvent ($\delta = 7.26$ for $CDCl_3$)[5]. ^{13}C NMR chemical shifts are reported in ppm relative to $SiMe_4$ ($\delta = 0$) and referenced internally with respect to solvent signal (δ 77.16 for $CDCl_3$)[5]. High-resolution mass spectrometry (HRMS) was conducted on an Agilent 6224 Accurate-Mass TOF LC/MS Mass Spectrometer using APCI ionization. Low-resolution mass spectroscopy (LRMS) was conducted on an Agilent 6120 Quadrupole LC/MS. Analytical thin layer chromatography (TLC) was performed on SorbTech polyester-backed 200 μm silica gel sheets. Preparative TLC was performed on SorbTech 1000 μm silica gel plates. Flash chromatography separations were conducted using silica gel 40-63 μm (230-400 mesh). Purification of compound **5c** was conducted on an Agilent 1260 system with UV-Vis detection, using a GEMINI C18 reverse phase column (10 ×150 mm, 5 μm particle size) and a gradient of 5% to 100% acetonitrile/water (+ 0.1% formic acid) over 15 min with a flow rate of 10 mL/min.

Synthesis of ethyl 8-ethoxy-4-oxo-4*H*-quinolizine-3-carboxylate, 1b

Sodium hydride (27 mg, 0.68 mmol, 60% dispersion in oil) was added portion-wise to 5 mL of absolute ethanol and stirred vigorously at R.T. until no gas evolution was observed. A solution of **1** (100 mg, 0.34 mmol) in 2 mL of dichloromethane was added, and the mixture was stirred at 50 °C for 2 h until TLC showed complete consumption of **1**. The resulting mixture was diluted with 30 mL of dichloromethane and washed with water, followed by brine. The aqueous fraction was extracted with dichloromethane and the combined organics were dried over Na_2SO_4 and evaporated. The residue was recrystallized from dichloromethane/diethyl ether to afford the product **1b** as a light yellow solid (76 mg, 86% yield). ^{1}H NMR (600 MHz, $CDCl_3$): δ 9.30 (d, *J*

= 7.9 Hz, 1H), 8.26 (d, *J* = 8.6 Hz, 1H), 6.81 (dd, *J* = 7.9, 2.7 Hz, 1H), 6.73 (d, *J* = 2.7 Hz, 1H), 6.41 (d, *J* = 8.6 Hz, 1H), 4.39 (q, *J* = 7.1 Hz, 2H), 4.19 (q, *J* = 7.0 Hz, 2H), 1.50 (t, *J* = 7.0 Hz, 3H), 1.40 (t, *J* = 7.1 Hz, 3H). $^{13}C\{^{1}H\}$ NMR (150 MHz, $CDCl_3$): δ 166.7, 162.9, 156.1, 148.7, 141.4, 131.6, 111.1, 103.3, 102.4, 100.8, 65.2, 60.7, 14.7, 14.4. HR-TOF-MS (*m/z*): $[M+H]^+$ calcd for $C_{14}H_{15}NO_4$, 262.1074; found 262.1079.

Synthesis of Ethyl-8-(diethylamino)-4-oxo-4H-quinolizine-3-carboxylate, 1c

Compound **1** (1.01 g, 3.97 mmol) and sodium bicarbonate (1.50 g, 17.9 mmol) were dissolved in dry acetonitrile (40 mL) under nitrogen. Diethylamine (3.00 mL, 28.8 mmol) was added dropwise to the reaction mixture. The resulting solution was allowed to stir for 48 h at 55 °C. The mixture was diluted with dichloromethane (330 mL) and washed with water (1×), then with 1M hydrochloric acid (1×) and with water again (2×). The organic phase was dried over $MgSO_4$ and solvent was evaporated under reduce pressure to afford the desired product as a yellow solid (1.04 g, 91% yield). ^{1}H NMR (400 MHz, $CDCl_3$, δ): 9.22 (d, *J* = 8.2 Hz, 1H), 8.08 (d, *J* = 8.9 Hz, 1H), 6.69 (dd, *J* = 8.2, 2.8 Hz, 1H), 6.34 (s, 1H), 6.22 (d, *J* = 8.9 Hz, 1H), 4.37 (q, *J* = 7.1 Hz, 2H), 3.49 (q, *J* = 7.1 Hz, 4H), 1.39 (t, *J* = 7.2 Hz, 3H), 1.27 (t, *J* = 7.2 Hz, 6H). $^{13}C\{^{1}H\}$ NMR (100 MHz, $CDCl_3$, δ): 167.5, 156.3, 150.5, 148.3, 139.8, 131.2, 105.7, 100.1, 98.8, 98.4, 60.2, 44.9, 14.8,12.6. ESI-MS (*m/z*): $[M+H]^+$ calcd for $C_{16}H_{20}N_2O_3$, 289.2; found 289.1.

Synthesis of ethyl 8-methoxy-4-oxo-4*H*-quinolizine-3-carboxylate, 1d

Sodium hydride (16 mg, 0.40 mmol, 60% dispersion in oil) was added portion-wise to 3 mL of methanol and stirred vigorously at R.T. until no gas evolution was observed. A solution of **2** (50 mg, 0.20 mmol) in 1 mL of dichloromethane was added, and the mixture was stirred at 50 °C for 2.5 h until TLC showed complete consumption of **2**. The resulting mixture was diluted with 20 mL of dichloromethane and washed with 20 mL of water, followed by brine. The aqueous fraction was extracted with dichloromethane and the combined organics were dried over Na_2SO_4 and evaporated to afford the product **1d** as a light orange solid (43 mg, 93% yield). ^{1}H NMR (600 MHz, $CDCl_3$): δ 9.33 (d, *J* = 8.0 Hz, 1H), 8.32 (d, *J* = 8.6 Hz, 1H), 6.87 (dd, *J* = 8.0, 2.6 Hz, 1H),

6.77 (d, J = 2.6 Hz, 1H), 6.48 (d, J = 8.6 Hz, 1H), 3.98 (s, 3H), 3.94 (s, 3H). $^{13}C\{^{1}H\}$ NMR (150 MHz, $CDCl_3$): δ 167.4, 163.8, 156.2, 148.9, 141.8, 131.7, 111.0, 103.3, 101.1, 56.5, 52.2, 29.9. ESI-MS (*m/z*): $[M+H]^+$ calcd for $C_{12}H_{11}NO_4$, 234.1; found 234.1.

Synthesis of ethyl 8-ethoxy-1-formyl-4-oxo-4*H*-quinolizine-3-carboxylate, 2b

Compound **1b** (65 mg, 0.25 mmol) was suspended in 1 mL of dry DMF and 0.30 mL of $POCl_3$ was added to the suspension dropwise at R.T. The resulting solution was stirred at R.T. for 2 h and poured into 20 mL of water to yield a precipitate. The pale-yellow product **2b** was collected via filtration, washed with abundant water and dried in vacuo (67 mg, 93% yield). ^{1}H NMR (600 MHz, $CDCl_3$): δ 9.79 (s, 1H), 9.39 (d, J = 7.9 Hz, 1H), 8.98 (d, J = 2.9 Hz, 1H), 8.67 (s, 1H), 7.04 (dd, J = 7.9, 2.9 Hz, 1H), 4.43 (q, J = 7.1 Hz, 2H), 4.36 (q, J = 7.0 Hz, 2H), 1.55 (t, J = 7.0 Hz, 3H), 1.42 (t, J = 7.1 Hz, 3H). $^{13}C\{^{1}H\}$ NMR (150 MHz, $CDCl_3$): δ 188.5, 167.5, 165.2, 155.1, 150.6, 147.9, 132.7, 112.5, 107.9, 103.5, 102.3, 66.3, 61.2, 14.6, 14.3. HR-TOF-MS (*m/z*): $[M+H]^+$ calcd for $C_{15}H_{15}NO_5$, 290.1023; found 290.1024.

Synthesis of Ethyl-8-(diethylamine)-1-formyl-4-oxo-4H-quinolizine-3-carboxylate, 2c

Compound **1c** (0.10 g, 0.35 mmol) was suspended in dry DMF (1.4 mL) and $POCl_3$ (55 μL, 0.45 mmol) was added dropwise to the suspension at R.T. The resulting solution was stirred at R.T. for 3 h and diluted with water (30 mL), followed by addition of saturated solution of sodium bicarbonate (30 mL). The reaction crude was extracted with ethyl acetate (3×) and the organic phase was dried over Na_2SO_4. The solvent was removed under vacuum to afford product **2c** as an orange solid (104 mg, 96.4% yield). ^{1}H NMR (400 MHz, $CDCl_3$, δ): 9.67 (s, 1H), 9.19 (d, J = 8.2 Hz, 1H), 8.64 (d, J = 3.0 Hz, 1H), 8.51 (s, 1H), 6.78 (dd, J = 8.2, 3.0 Hz, 1H), 4.40 (q, J = 7.1 Hz, 2H), 3.60 (q, J = 7.1 Hz, 4H), 1.41 (t, J = 13.9 Hz, 3H), 1.33 (t, J = 13.9 Hz, 6H). $^{13}C\{^{1}H\}$ NMR (100 MHz, $CDCl_3$, δ): 188.2, 165.8, 155.7, 153.6, 151.6, 145.3, 132.0, 107.6, 106.0, 100.3, 99.2, 60.8, 45.5, 14.7, 12.3. ESI-MS (*m/z*): $[M+H]^+$ calcd for $C_{17}H_{20}N_2O_4$, 317.2; found 317.1.

Synthesis of ethyl 1-(hydroxymethyl)-4-oxo-4*H*-quinolizine-3-carboxylate, 3a

Compound **2a** (0.30 g, 1.2 mmol) was suspended in 40 mL of ethanol, cooled in an ice bath and treated with $NaBH_4$ (0.14 g, 3.7 mmol) was added to the suspension. The mixture was stirred for 90 min at 0 °C until TLC showed complete consumption of **2a**. The resulting mixture was poured carefully into water and extracted with dichloromethane. The organic fraction was dried over Na_2SO_4 and evaporated to afford product **3a** as a bright yellow solid (0.28 g, 93% yield). ^{1}H NMR (400 MHz, $CDCl_3$): δ 9.33-9.31 (m, 1H), 8.14 (s, 1H), 8.10-8.08 (m, 1H), 7.72-7.68 (m, 1H), 7.22-7.18 (m, 1H), 4.81 (s, 2H), 4.32 (q, *J* = 7.1 Hz, 2H), 3.31 (s, 1H), 1.39 (t, *J* = 7.1 Hz, 3H). ^{13}C{^{1}H} NMR (150 MHz, $CDCl_3$): δ 165.9, 155.7, 145.3, 141.4, 134.4, 130.0, 123.4, 117.1, 112.9, 104.7, 62.6, 61.0, 14.5. HR-TOF-MS (*m/z*): $[M+H]^+$ calcd for $C_{13}H_{13}NO_4$, 248.0917; found 248.0916.

Synthesis of ethyl 8-ethoxy-1-(hydroxymethyl)-4-oxo-4*H*-quinolizine-3-carboxylate, 3b

Compound **2b** (60 mg, 0.21 mmol) was suspended in 5 mL of ethanol, cooled in an ice bath and treated with $NaBH_4$ (24 mg, 0.62 mmol). The mixture was stirred for 2 h at 0 °C until TLC showed complete consumption of **7**. The resulting mixture was poured carefully into water and extracted with dichloromethane. The organic fraction was dried over Na_2SO_4 and evaporated to afford product **3b** as a yellow solid (58 mg, 96% yield). ^{1}H NMR (600 MHz, $CDCl_3$): δ 9.21 (d, *J* = 8.0 Hz, 1H), 7.96 (s, 1H), 7.28 (d, *J* = 2.7 Hz, 1H), 6.82 (dd, *J* = 7.9, 2.8 Hz, 1H), 4.73 (d, *J* = 5.9 Hz, 2H), 4.30-4.26 (m, 4H), 3.25-3.24 (m, 1H), 1.52 (t, *J* = 7.0 Hz, 3H), 1.38 (t, *J* = 7.1 Hz, 3H). ^{13}C{^{1}H} NMR (150 MHz, $CDCl_3$): δ 166.1, 163.5, 155.8, 148.0, 141.2, 132.0, 111.2, 111.1, 101.3, 101.1, 65.5, 63.2, 60.6, 14.6, 14.4. HR-TOF-MS (*m/z*): $[M+H]^+$ calcd for $C_{15}H_{17}NO_5$, 292.1179; found 292.1183.

Synthesis of ethyl-8-(diethylamine)-1-hydroxymethyl-4-oxo-4H-quinolizine-3-carboxylate, 3c

Compound **2c** (87 mg, 0.28 mmol) was suspended in ethanol (5.6 mL), cooled in an ice bath and treated with NaBH4 (35 mg, 0.84 mmol). The mixture was stirred for 1.5 hours at 0° C until TLC showed complete consumption of **2c**. The mixture was diluted in dichloromethane (50 mL) and

washed with water (2×) and brine (1×). The organic fraction was dried over Na2SO4 and evaporated to afford product **3c** as a bright yellow solid (0.0786 g, 90.0% yield). ^{1}H NMR (400 MHz, CDCl3, δ): 9.18 (d, *J* = 8.2 Hz, 1H), 7.88 (s, 1H), 6.85 (d, *J* = 2.5 Hz, 1H), 6.69 (dd, *J* = 8.2, 2.5 Hz, 1H), 4.68 (s, 2H), 4.29 (q, *J* = 7.1 Hz, 2H), 3.54 (q, *J* = 7.1 Hz, 4H), 1.36 (t, *J* = 7.1 Hz, 3H), 1.29 (t, *J* = 7.1 Hz, 6H). ^{13}C{^{1}H} NMR (100 MHz, $CDCl_3$, δ): 167.2, 156.1, 150.9, 147.1, 139.9, 131.8, 109.7, 105.6, 97.7, 96.7, 63.7, 60.2, 45.1, 14.7, 12.6. ESI-MS (m/z): $[M+H]^+$ calcd for $C_{17}H_{22}N_2O_4$, 319.2; found 319.1.

Synthesis of ethyl 1-(azidomethyl)-4-oxo-4*H*-quinolizine-3-carboxylate, 4a

Compound **3a** (0.10 g, 0.4 mmol) was suspended in 30 mL of toluene under N_2 atmosphere, cooled in an ice bath, and treated with diphenyl phosphoryl azide (0.17 g, 0.6 mmol). DBU (0.09 g, 0.6 mmol) was added to the suspension and the mixture was stirred at 0 °C for 1 h, then at room temperature overnight. The resulting mixture was evaporated and the residue was purified by column chromatography (silica gel, 2:1 dichloromethane/acetone, v/v) to afford product **4a** as a bright yellow solid (0.10 g, 93% yield). ^{1}H NMR (400 MHz, $CDCl_3$): δ 9.55-9.53 (m, 1H), 8.40 (s, 1H), 7.86-7.78 (m, 2H), 7.35-7.31 (m, 1H), 4.54 (s, 2H), 4.43 (q, *J* = 7.1 Hz, 2H), 1.43 (t, *J* = 7.1 Hz, 3H). ^{13}C{^{1}H} NMR (150 MHz, $CDCl_3$): δ 166.0, 155.6, 145.3, 142.9, 135.3, 130.9, 122.3, 117.2, 106.2, 105.4, 61.2, 52.0, 14.6. HR-TOF-MS (*m/z*): $[M+H]^+$ calcd for $C_{13}H_{12}N_4O_3$, 273.0982; found 273.0985.

Synthesis of ethyl 1-(azidomethyl)-8-ethoxy-4-oxo-4*H*-quinolizine-3-carboxylate, 4b

Compound **3b** (50 mg, 0.17 mmol) was suspended in 15 mL of toluene under N_2 atmosphere, cooled in an ice bath and treated with diphenyl phosphoryl azide (71 mg, 0.26 mmol). DBU (39 mg, 0.26 mmol) was added to the suspension and the mixture was stirred at 0 °C for 1 h, then at room temperature overnight and 50 °C for 5 h. The resulting mixture was evaporated, and the residue was purified by column chromatography (silica gel, 1:1 dichloromethane/acetone, v/v) to afford product **4b** as a yellow solid (44 mg, 81% yield). ^{1}H NMR (600 MHz, $CDCl_3$): δ 9.44 (dd, *J* = 6.6, 2.0 Hz, 1H), 8.28 (s, 1H), 6.94-6.93 (m, 2H), 4.44 (s, 2H), 4.41 (q, *J* = 7.1 Hz, 2H), 4.28

(q, J = 7.0 Hz, 2H), 1.54 (t, J = 7.0 Hz, 3H), 1.42 (t, J = 7.1 Hz, 3H). $^{13}C\{^{1}H\}$ NMR (150 MHz, $CDCl_3$): δ 166.4, 164.2, 155.7, 147.9, 143.2, 133.0, 111.0, 104.2, 101.8, 100.2, 65.6, 60.9, 52.6, 14.7, 14.4. HR-TOF-MS (*m/z*): $[M+H]^+$ calcd for $C_{15}H_{16}N_4O_4$, 317.1244; found 317.1246.

Synthesis of ethyl-1-(azidomethyl)-8-(diethylamino)-4-oxo-4H-quinolizine-3-carboxylate, 4c

Compound **3c** (46 mg, 0.16 mmol) was suspended in toluene (16 mL) under N_2 atmosphere, cooled in an ice bath and treated with diphenyl phosphoryl azide (53 µL, 0.235 mmol). DBU (36 µL, 0.235 mmol) was added to the suspension and the mixture was allowed to stir at 0° C for 1 h, then raised to 50° C and stirred overnight. The resulting mixture was evaporated, and the residue was purified by preparative TLC on silica gel (2:1 dichloromethane/acetone) to afford product **4c** as a light yellow solid (203 mg, 41.4% yield). ^{1}H NMR (400 MHz, $CDCl_3$, δ): 9.32 (d, J = 8.1 Hz, 1H), 8.11 (s, 1H), 6.77 (d, J = 7.1 Hz, 1H), 6.51 (s, 1H), 4.40 (q, J = 7.0 Hz, 4H), 3.56 (q, J = 7.0 Hz, 4H), 1.41 (t, J = 7.0 Hz, 3H), 1.31 (t, J= 7.0 Hz, 6H). $^{13}C\{^{1}H\}$ NMR (100 MHz, $CDCl_3$, δ): 167.2, 156.1, 151.2, 146.8, 141.9, 132.4, 105.7, 103.1, 97.1, 96.6, 60.5, 53.3, 45.3, 14.8, 12.5. ESI-MS (*m/z*): $[M+H]^+$ calcd for $C_{17}H_{21}N_5O_3$, 344.2; found 344.1.

Synthesis of Eu(III) complex 5a

A mixture of Eu(III) complex **8** (50 mg, 85 µmol), **4a** (15 mg, 55 µmol), $CuSO_4 \cdot 5H_2O$ (5 mg, 20 µmol) and sodium ascorbate (8 mg, 40 µmol) was suspended in a 2:1 mixture of acetonitrile/water (3 mL). The suspension was then treated with triethylamine (30 µL) and stirred at R.T. overnight. The resulting mixture was evaporated, and the residue was re-suspended in water (1 mL). The suspension was centrifuged, and the supernatant was purified by reversed phase HPLC to afford product **5a** as a yellow solid (10 mg, 21% yield). HR-TOF-MS (*m/z*): $[M+H]^+$ calcd for $C_{32}H_{40}EuN_9O_{10}$, 864.2200; found 864.2188.

Synthesis of Eu(III) complex 5b

A mixture of Eu(III) complex **8** (40 mg, 68 µmol), **4b** (15 mg, 47 µmol), $CuSO_4 \cdot 5H_2O$ (5 mg, 20 µmol) and sodium ascorbate (8 mg, 40 µmol) was suspended in a 2:1 mixture of acetonitrile/water

(3 mL). The suspension was then treated with triethylamine (30 µL) and stirred at R.T. overnight. The resulting mixture was purified by reversed phase preparative TLC (C18 silica gel, 1:1 acetonitrile/water, v/v) to afford product **5b** as yellow solid. (12 mg, 28% yield) HR-TOF-MS (*m/z*): $[M+H]^+$ calcd for $C_{34}H_{44}EuN_9O_{11}$, 908.2462; found 908.2450.

Synthesis of Eu(III) complex 5c

A mixture of Eu(III) complex **8** (39 mg, 66 µmol), compound **4c** (15 mg, 44 µmol), $CuSO_4 \cdot 5H_2O$ (11 mg, 44 µmol) and sodium ascorbate (18 mg, 87 µmol) was suspended in a 2:1 mixture of acetonitrile/water (2.5 mL). The suspension was then treated with triethylamine (30 µL) and stirred at room temperature overnight. The resulting mixture was passed through a plug of reverse phase silica to remove the copper sulfate, and solvent was removed under vacuum. The residue was purified by semi-preparative C-18 reversed phase HPLC using a gradient of 5% to 100% acetonitrile/water (+ 0.1% formic acid) to afford product **5c** as a light yellow solid (4.33 mg, 10.6% yield). ESI-MS (*m/z*): $[M+H]^+$ calcd for $C_{36}H_{49}EuN_{10}O_{10}$, 935.2; found 935.3. HR-TOF-MS (m/z): $[M+H]^+$ calcd for $C_{36}H_{49}EuN_{10}O_{10}$, 935.2946; found 935.2926.

Synthesis and preparation of quantitative solutions of MagQEu1

Compound **5a** (1.74 mg, 2.0 µmol) was dissolved in 100 µL of methanol, treated with 100 µL of 1 M aqueous NaOH solution and stirred vigorously at R.T. for 1 h. The resulting mixture was neutralized with 1 M HCl solution, quantitatively transferred to a volumetric flask, and diluted with water to a final volume of 2.0 mL. An aliquot of the solution was analyzed by HPLC and high-resolution mass spectra to confirm quantitative hydrolysis. The resulting stock solution of **MagQEu1** was divided into small aliquots, flash frozen and stored at -20 °C until use. HR-TOF-MS (*m/z*): $[M+H]^+$ calcd for $C_{30}H_{36}EuN_9O_{10}$, 836.1887; found 836.1883.

Synthesis of MagQEu2

A sample of **5b** (1.8 mg, 2.0 µmol) was dissolved in 100 µL of methanol, and treated with 100 µL of 1 M aqueous NaOH solution and stirred vigorously at 50 °C overnight. The resulting mixture

was neutralized with 1 M HCl solution and purified by reversed phase preparative TLC (C18 silica gel, 100:100:1 acetonitrile/water/triethylamine) to afford **MagQEu2** as yellow solid (0.6 mg, 35% yield). HR-TOF-MS (*m/z*): $[M-H]^-$ calcd for $C_{31}H_{38}EuN_9O_{11}$, 864.1847; found 864.1821.

Synthesis and preparation of quantitative solutions of MagQEu3

Compound **5c** (0.96 mg, 1.1 μmol) was dissolved in methanol (100 μL) and treated with 1 M aqueous NaOH (100 μL) and stirred vigorously at 50 °C for 4 h. The resulting mixture was quantitatively transferred to a volumetric flask and diluted with 50 mM PIPES 100 mM KCl (pH = 7.0) to a final volume of 2.0 mL. An aliquot of the solution was analyzed by HPLC and high-resolution mass spectrometry to confirm quantitative hydrolysis. The resulting stock solution of **MagQEu3** was divided into small aliquots, flash frozen and stored at -20 °C until use. ESI-MS (*m/z*): $[M+H]^+$ calcd for $C_{34}H_{45}EuN_{10}O_{10}$, 907.3; found 907.3. HR-TOF-MS (m/z): $[M+Na]^+$ calcd for $C_{34}H_{45}EuN_{10}O_{10}$, 929.2428; found 929.2438.

Synthesis of 8-(diethylamino)-4-oxo-4H-quinolizine-3-carboxylic acid, 6c

Compound **1c** (10 mg, 35 μmol) was dissolved in methanol (500 μL), treated with 1 M aqueous NaOH (107 μL) and stirred vigorously at 50 °C for 23 hours. An aliquot of the solution was analyzed by HPLC and high-resolution mass spectrometry to confirm quantitative hydrolysis. The organic solvent was removed under vacuum, affording a yellow solid. The solid was dissolved in water (500 μL), cooled to 0 °C, and solution was acidified using 3 M HCl (54 μL). The suspension was filtered, and the yellow wet solid was lyophilized, affording compound **6c** as a yellow solid. (7.2 mg, 77.5% yield).

Synthesis of 8-methoxy-4-oxo-4*H*-quinolizine-3-carboxylic acid, 6d

Compound **1d** (15 mg, 64 μmol) was dissolved in methanol (560 μL), treated with 1 M aqueous NaOH (193 μL) and stirred vigorously at 50 °C for 6 hours. An aliquot of the solution was analyzed by HPLC and high-resolution mass spectrometry to confirm quantitative hydrolysis. The organic solvent was removed under vacuum, affording an orange solid. The solid was dissolved in water

(560 µL), cooled to 0 °C, and solution was acidified using 3 M HCl (70 µL). The suspension was filtered, and the wet light orange solid was lyophilized, affording compound **6d** as a light orange solid. (12.3 mg, 87% yield).

Synthesis of ethyl-8-(diethylamine)-1-hydroxymethyl-4-oxo-4H-quinolizine-3-carboxylic acid, 7c

Compound **3c** (5.53 mg, 17 µmol) was dissolved in methanol (438 µL), treated with 0.25 M KOH (438 µL) and stirred vigorously overnight at 50 °C. The organic solvent was removed under vacuum and the crude mixture was diluted with 3.50 mL of 50 mM PIPES 100 mM KCl (pH = 8.0). An aliquot of the solution was analyzed by HPLC and high-resolution mass spectrometry to confirm quantitative hydrolysis. The resulting stock solution was divided into small aliquots, flash frozen and stored at -20 °C until use. ESI-MS (*m/z*): $[M+H]^+$ calcd for $C_{15}H_{18}N_2O_4$, 291.1; found 291.2.

S2.2 Spectroscopic Measurements

All aqueous solutions were prepared using de-ionized water with resistivity of 18 MΩ·cm. Other solvents were supplied by commercial vendors and used as received. Organic buffers, 99.999% KCl, 99.999% $MgCl_2$, high-purity 25% HCl, KOH, adenosine 5′-triphosphate disodium salt hydrate (≥99%), cytidine 5′-triphosphate disodium salt (97%), uridine 5′-triphosphate trisodium salt (98%), guanosine 5′-triphosphate disodium salt (98%), thymidine 5’-triphosphate sodium salt (≥96%) and deoxyribonucleic acid sodium salt from calf thymus (type I, fibers) were purchased from Sigma Aldrich or Alfa Aesar. Measurements at pH 7.0 were conducted in aqueous buffer containing 50 mM PIPES and 100 mM KCl previously treated with Chelex resin (Bio-Rad) according to the manufacturer’s protocol, to remove divalent metal ions. Measurements of pH were conducted using a Mettler Toledo FE20 pH meter with glass electrode. Absorption spectra were obtained using a Cary 100 UV-VIS Spectrophotometer by Agilent Technologies. Steady-state spectra were collected on a QuantaMaster 40 Photon Technology International spectrofluorometer equipped with Xenon lamp source, emission and excitation monochromators,

excitation correction unit, and PMT detector. All measurements were conducted at 25.0 ± 0.1 °C maintained by a Quantum Northwest cuvette temperature controller. Emission and excitation spectra were corrected for the detector wavelength-dependent response and wavelength-dependent lamp intensity. Time-resolved luminescence decays were measured using a QuantaMaster-8075-21 (Horiba) spectrophotometer. Samples were excited at 388 nm with double monochromator filtered emission from a pulsed Xe-arc lamp (frequency: 300 MHz) and luminescence was detected using a PMT detector. Decay traces were fitted to a first order exponential decay function in OriginPro. Time-gated luminescence spectra were acquired on a FlexStation 3 Multi-Mode Microplate Reader from Molecular Devices. The integration delay was set to 0.1 ms with an integration time of 1 ms. The wavelength step was set to 1 nm for acquiring the luminescence spectra of each probe. All measurements were conducted at 25.0 ± 0.1 °C, using a concentration of 5 μM of the probe unless otherwise noted.

Preparation of quantitative solutions of nucleoside triphosphates

A sample of nucleoside triphosphate sodium salt (0.1 mmol) was dissolved in de-ionized water and the pH of the solution was adjusted to 7.0 by careful addition of a concentrated KOH solution. The resulting mixture was transferred quantitatively to a volumetric flask and diluted with water to a final volume of 1.0 mL. The stock solution (100 mM) was divided into small aliquots, flash frozen and stored at -20 °C until use. Stock solutions in deuterated buffer were prepared in a similar fashion, using deuterated solvents and reagents.

Preparation of quantitative solutions of DNA

Deoxyribonucleic acid sodium salt from calf thymus (7.8 mg, 41.9 mol % G-C and 58.1 mol % A-T) was treated with 1.5 mL of de-ionized water. The mixture was gently shaken at 4 °C overnight for complete dissolution of the DNA sample. An aliquot of the solution was diluted in de-ionized water and the absorbance at 260 nm was measured by UV-Vis spectrophotometer. Concentration of the phosphate in DNA solution in molarity, [P], was estimated based on the calculated average

extinction coefficient of the nucleobase in aqueous solution at 260 nm, assuming [nucleobase] = [P]. The stock solution (10.8 mM) was stored at -20 °C until use.

Luminescence experiments with MgNTPs

For steady-state fluorescence and time-resolved luminescence experiments MgNTP, complexes were generated *in situ* by combining $MgCl_2$ and the nucleoside triphospate in a 1:1 Mg^{2+}/nucleobase ratio in water at pH = 7.0.

Luminescence lifetime measurements

For lifetime data acquisition, MagQEu1 was excited at 388 nm and Eu^{3+} luminescence was collected at 700 nm. Measurements were conducted using solutions of 50 μM sensor in the presence and absence of 50 mM $MgCl_2$ or 50 mM MgATP in protio or deutero PIPES buffer (50 mM, 100 mM KCl, pH 7 or pD 7.12). Stock solutions of sensor and MgATP were thawed immediately before the experiment.

Solutions in deuterated buffer: Deuterated PIPES was prepared by lyophilizing PIPES buffer (5 mL) and redissolving the residue in deuterium oxide (5 mL). A stock solution of MagQEu1 (1 mM) in deuterated PIPES was prepared by lyophilizing 100 μL of 1 mM solution in protio buffer and redissolving the residue in D_2O (100 μL). Solutions of MgNTPs in deuterated buffer were prepared by combining $MgCl_2$ (in D_2O) and the nucleoside triphosphate in a 1:1 Mg^{2+}/nucleobase ratio at pD = 7.12.

Simultaneous detection of free and biomolecule-bound Mg^{2+} with MagQEu3 and MagB2

Samples in aqueous buffer (PIPES 50 mM, KCl 100 mM, pH 7.0) were prepared containing a mixture of MagB2[6] (5 μM) and MagQEu3 (5 μM); a mixture of MagB2 (5 μM), MagQEu3 (5 μM) and MgCl2 (5 mM); a mixture of MagB2 (5 μM), MagQEu3 (5 μM) and MgATP (5 mM); and a mixture of MagB2 (5 μM), MagQEu3 (5 μM), MgCl2 (5 mM) and MgATP (5 mM). Measurements of fluorescence (MagB2, λ_{exc}= 575 nm, λ_{em} = 602 nm) and time-gated luminescence

(MagQEu3, Mg^{2+}-bound, λ_{exc}= 391 nm, λ_{em}= 592 nm) were carried out in a FlexStation 3 Multi-Mode Microplate Reader. Solutions equilibrated for 30 min prior to measurement.

S2.3 Determination of dissociation constants

Fluorescence and time-gated luminescence titrations with Mg^{2+} and nucleoside triphosphate-bound Mg^{2+} were conducted using 5 μM solutions of the sensor in aqueous buffer at pH 7.0. Additions from a 100 mM $MgCl_2$ solution were used to adjust the total concentration of Mg^{2+} from 0 to 60 mM in the cuvette or 0 to 25 mM in the half-well 96-wellplate. Additions from a 100 mM nucleoside triphosphate solution and a 100 mM $MgCl_2$ solution were used to adjust the total concentration of nucleoside triphosphate-bound Mg^{2+} in one-to-one ratio from 0 to 25 mM in the cuvette. For each fluorescence titration, the Mg^{2+} solution was treated with an appropriate amount of the sensor to match the concentration in the cuvette and prevent sensor dilution throughout the experiment. Apparent K_d values for Mg^{2+} dissociation were obtained from non-linear plots using equation S1, where I_{min} is the integrated fluorescence or luminescence emission of the metal-free sensor and I_{max} is the integrated fluorescence or luminescence emission of the metal-saturated sensor. The approximation $[Mg^{2+}] \approx [Mg^{2+}]_t$ was made.

$$\left[Mg^{2+}\right]=K_d \frac{I-I_{min}}{I_{max}-I} \qquad \text{(Equation S1)}$$

Apparent K_d values for nucleoside triphosphate-bound Mg^{2+} were also obtained from non-linear plots using equation S1 based on a ternary probe·Mg·nucleoside triphosphate complex model.

S2.4 Electrochemical Studies

Cyclic and linear sweep voltammetry studies were performed using CH Instrument potentiostat model 400A, using a three-cell-electrode arrangement consisting of a Platinum working electrode, a thin Pt wire counter electrode and a non-aqueous $Ag/AgNO_3$ reference electrode, all purchased from CH Instruments. Measurements were performed using a 1 mM solution of each antenna in acetonitrile containing 0.1 M tetra-*n*-butylammonium hexafluorophosphate (Bu_4NPF_6) as

supporting electrolyte. Prior to each experiment, the working electrode was cleaned by polishing with 0.3 μm and 0.05 μm alumina, followed by sonication in water and ethanol. For reversible peaks, the half-wave potential was obtained by taking the mean of the anodic and cathodic peak potentials. For irreversible peaks, the peak potential was reported. Both positive and negative scans were collected at 150 mV/s for each chelator, and identical electrochemical responses were obtained in both directions. Ferrocene (5 mM) was added as an internal reference (0.40 V vs. SCE)[7] and potentials were reported vs. Standard Calomel Electrode (SCE).

S3. Characterization of new compounds

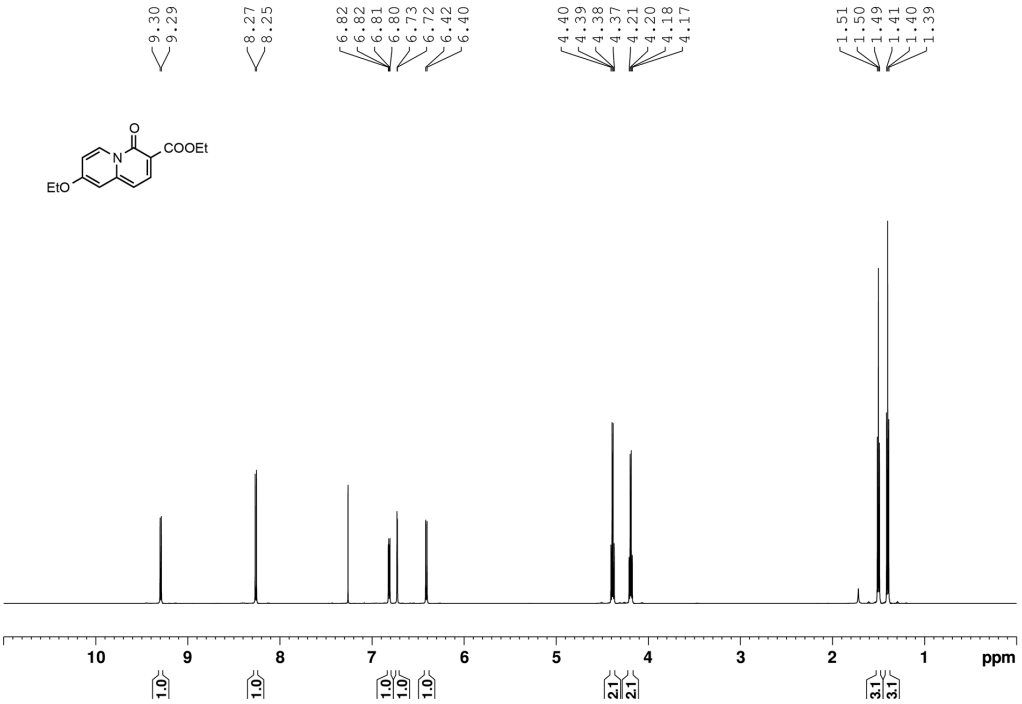

Figure S16. ^{1}H NMR spectrum of **1b** in $CDCl_3$

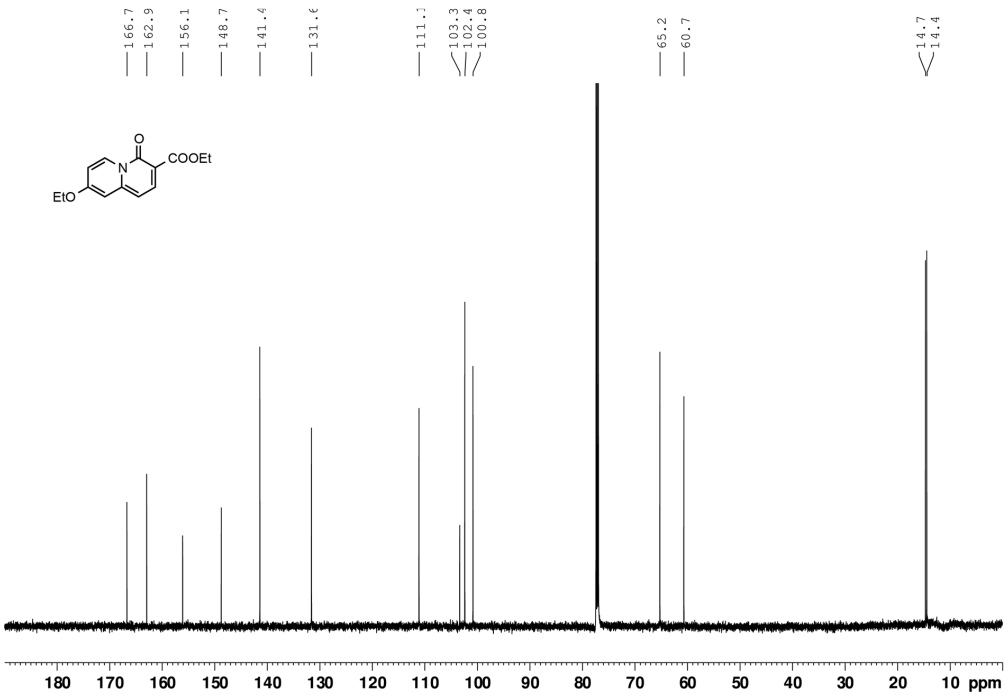

Figure S17. $^{13}C\{^{1}H\}$ NMR spectrum of **1b** in $CDCl_3$.

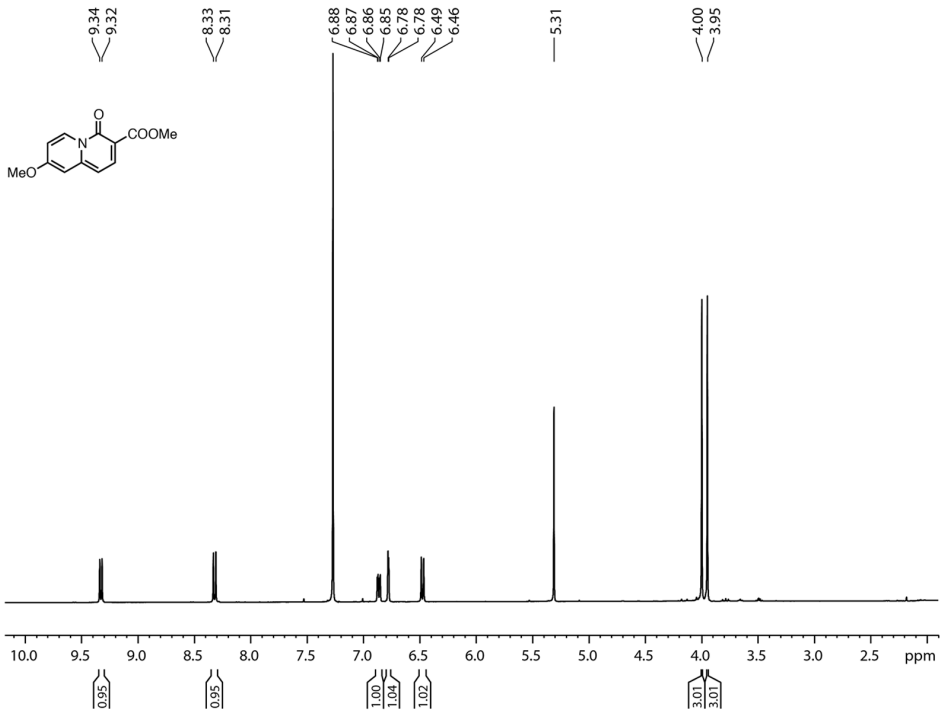

Figure S18. ^{1}H NMR spectrum of **1d** in $CDCl_3$.

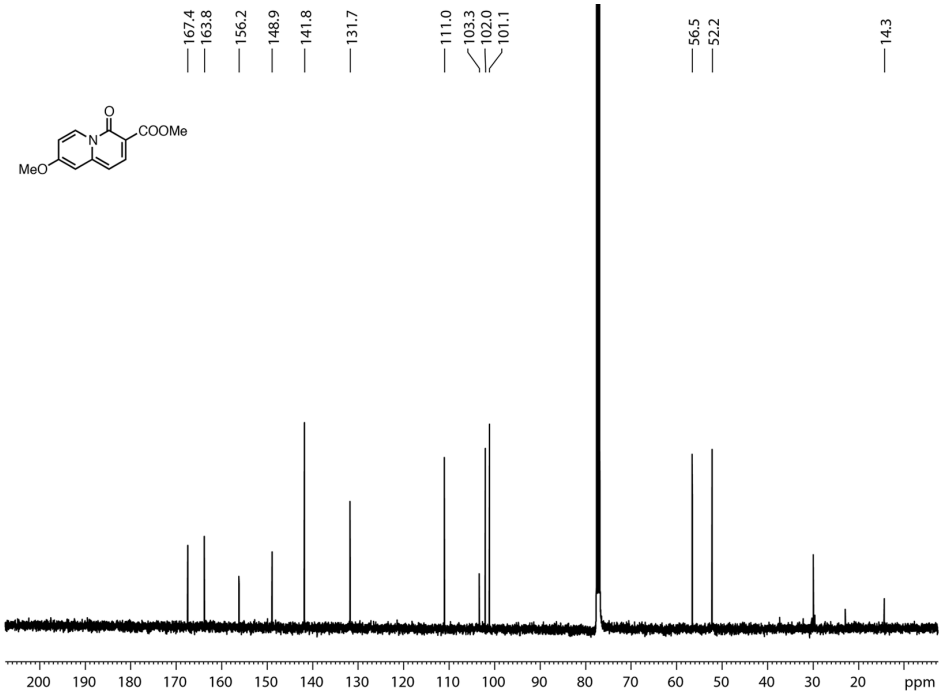

Figure S19. $^{13}C\{^{1}H\}$ NMR spectrum of **1d** in $CDCl_3$.

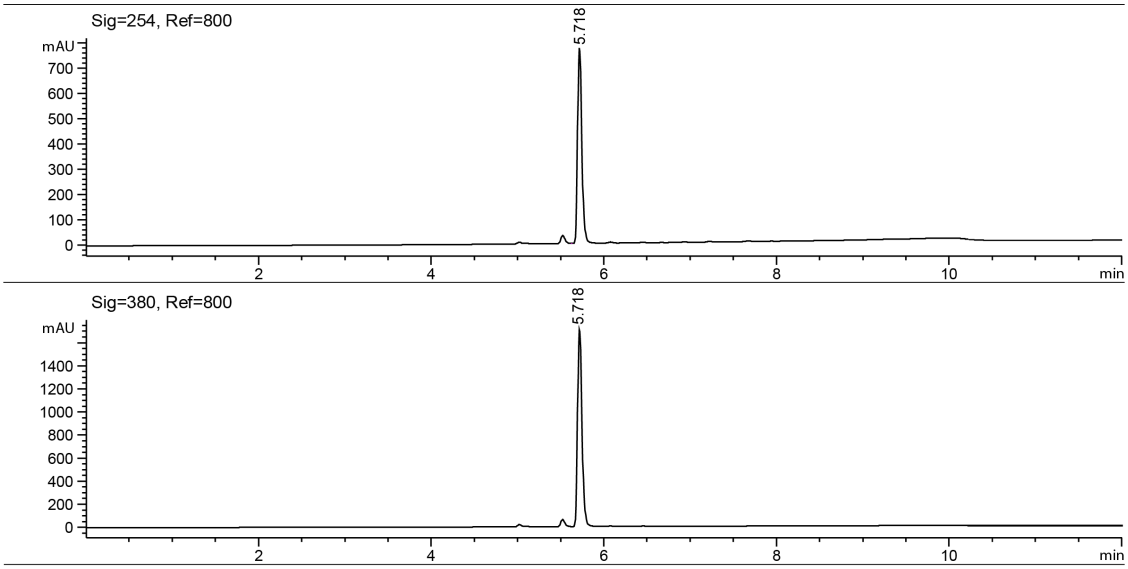

Figure S20. Reversed phase HPLC chromatogram of **1d**, eluted with 10% to 100% acetonitrile/ water (+0.1% TFA) gradient.

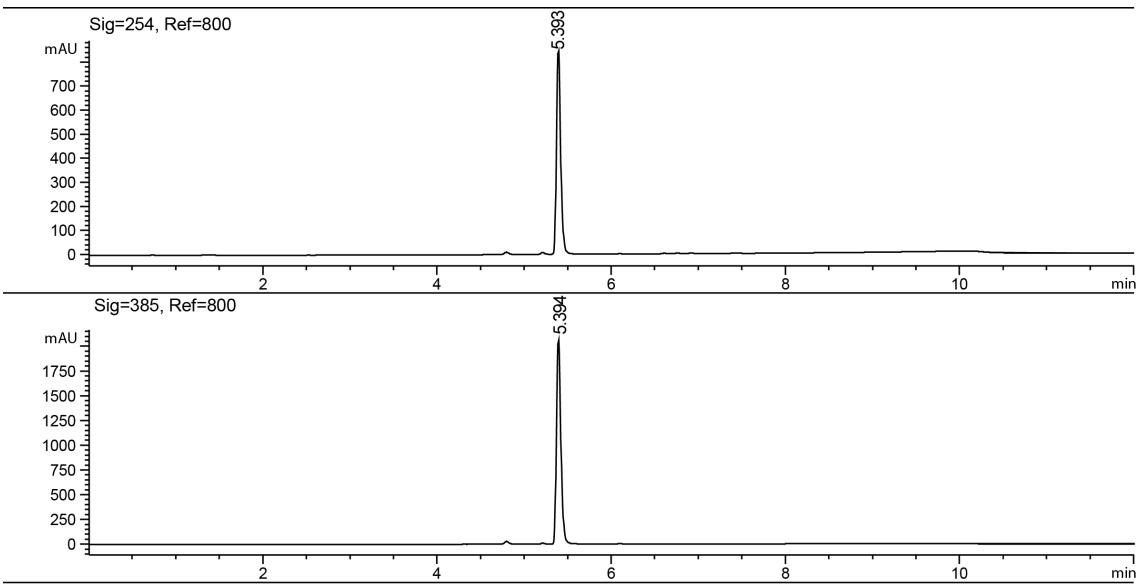

Figure S21. Reversed phase HPLC chromatogram of **6d**, eluted with 10% to 100% acetonitrile/ water (+0.1% TFA) gradient.

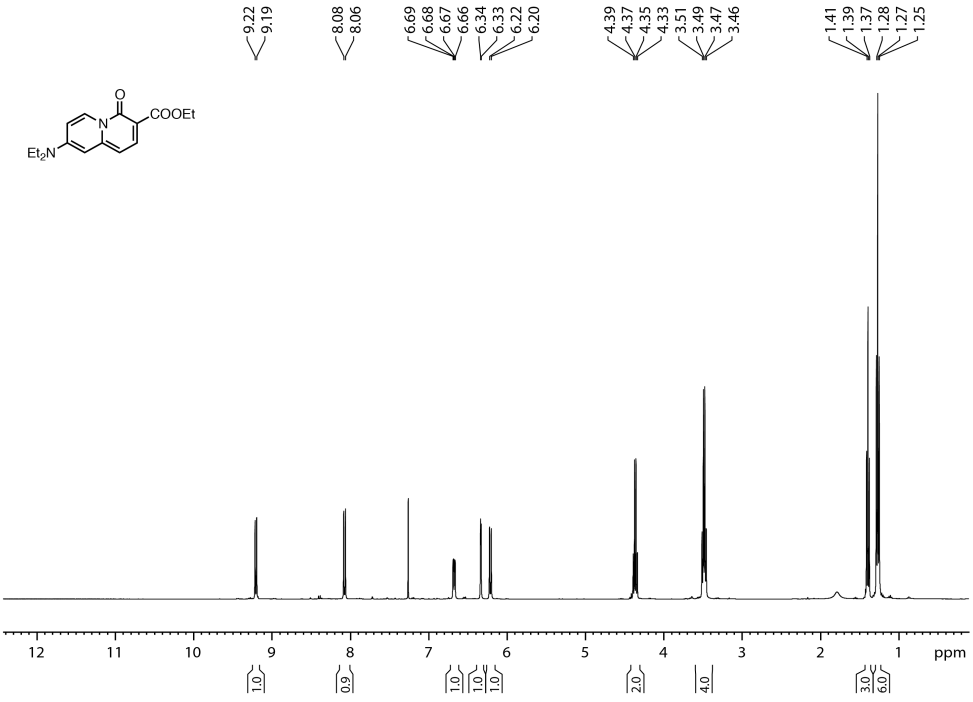

Figure S22. ^{1}H NMR spectrum of **1c** in $CDCl_3$

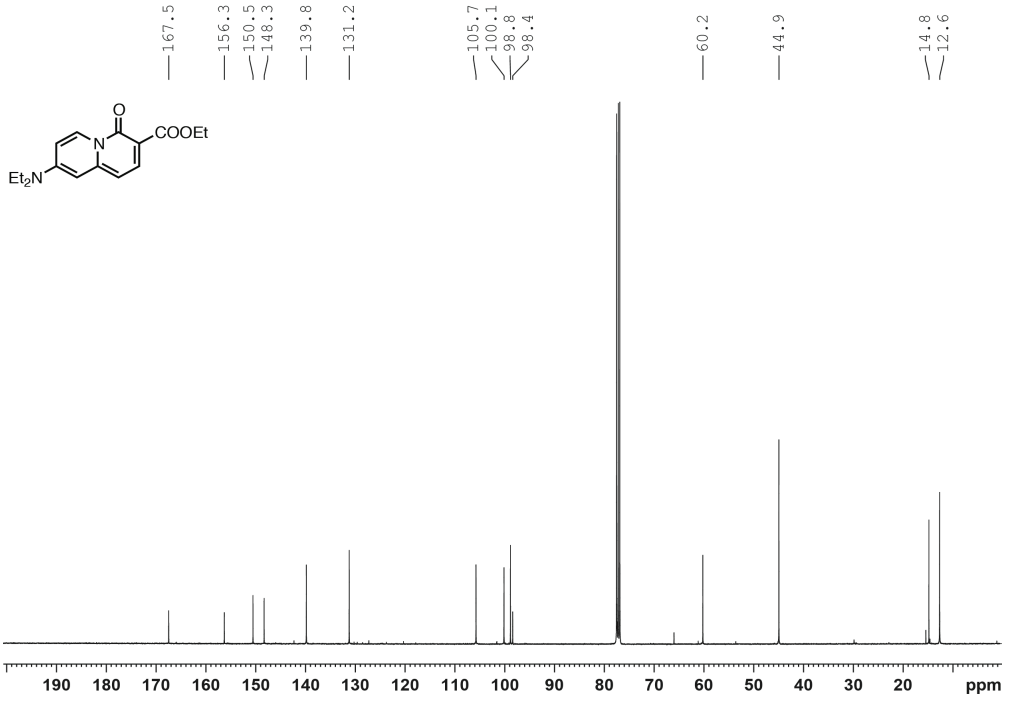

Figure S23. $^{13}C\{^{1}H\}$ NMR spectrum of **1c** in $CDCl_3$

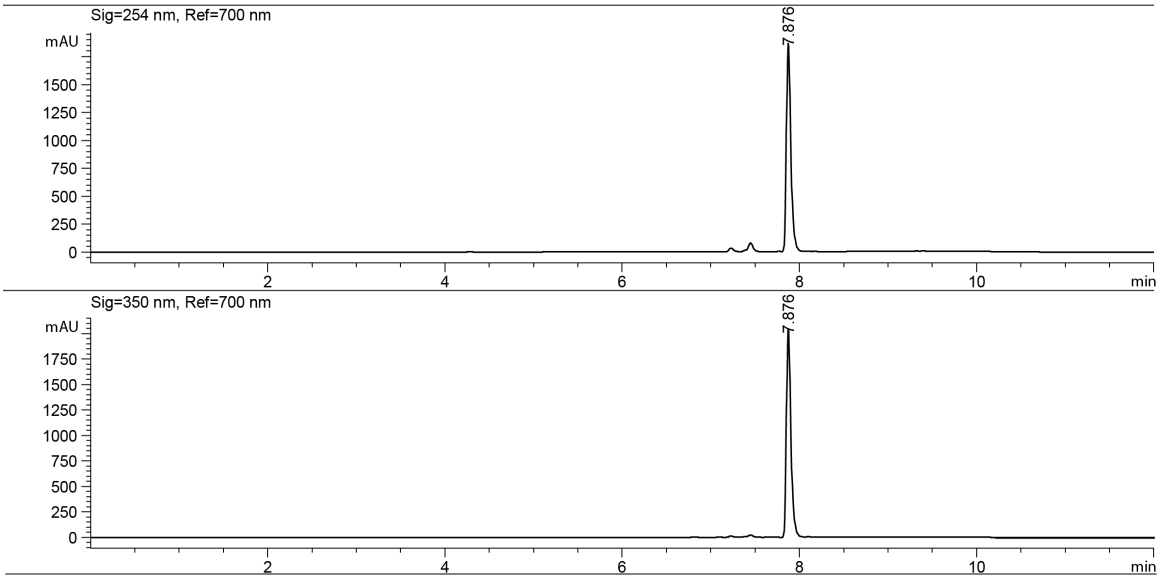

Figure S24. Reversed phase HPLC chromatogram of **1c**, eluted with 10% to 100% acetonitrile/ water (+0.1% TFA) gradient.

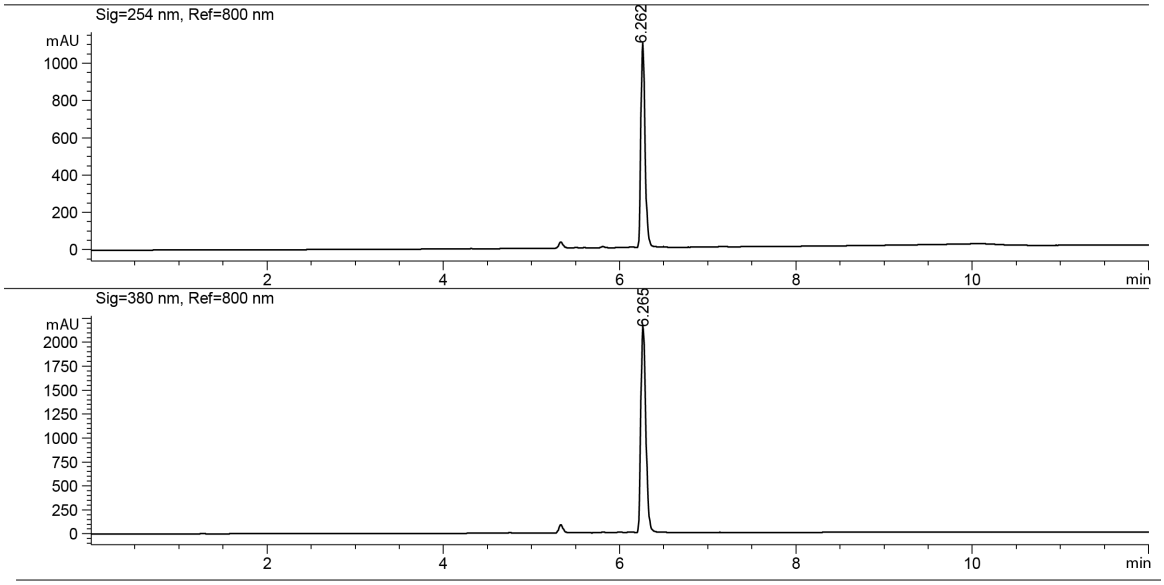

Figure S25. Reversed phase HPLC chromatogram of **6c**, eluted with 10% to 100% acetonitrile/ water (+0.1% TFA) gradient.

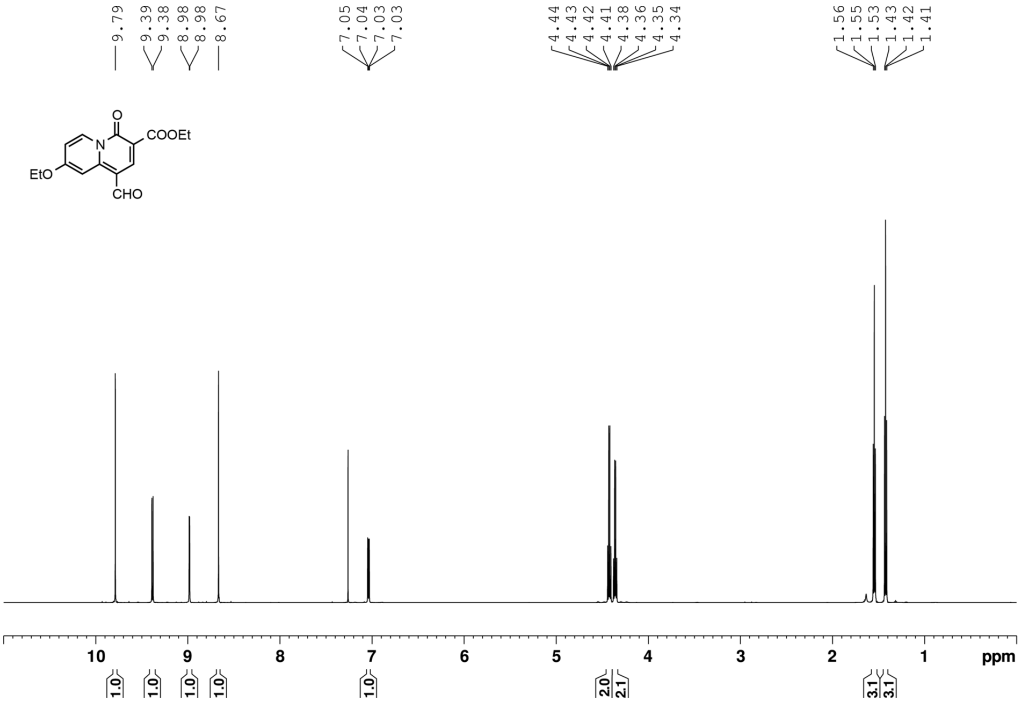

Figure S26. ^{1}H NMR spectrum of **2b** in $CDCl_3$

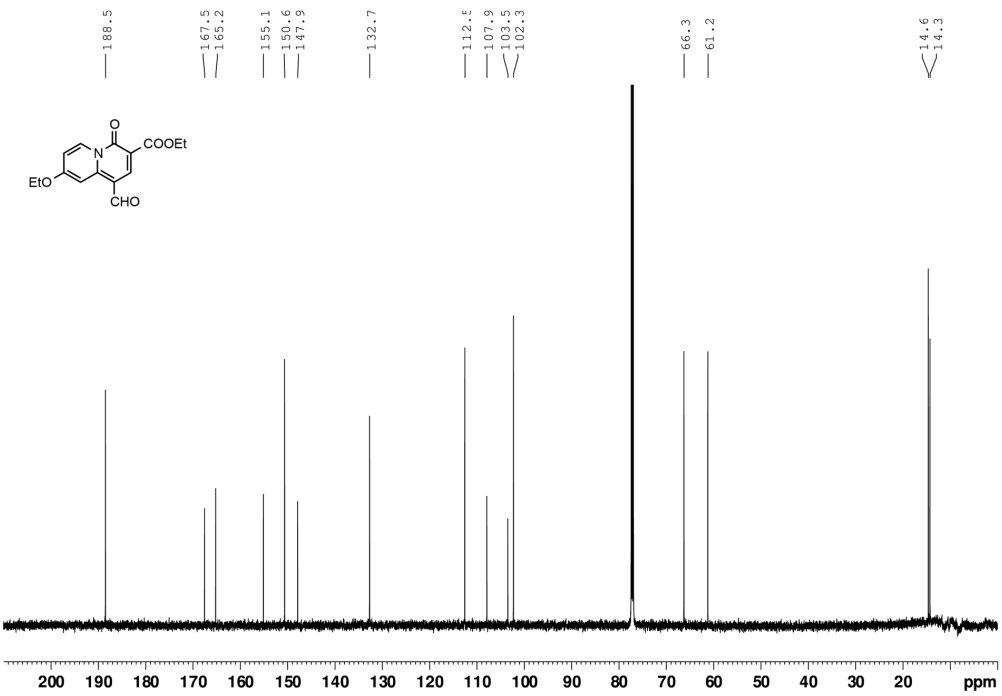

Figure S27. $^{13}C\{^{1}H\}$ NMR spectrum of **2b** in $CDCl_3$

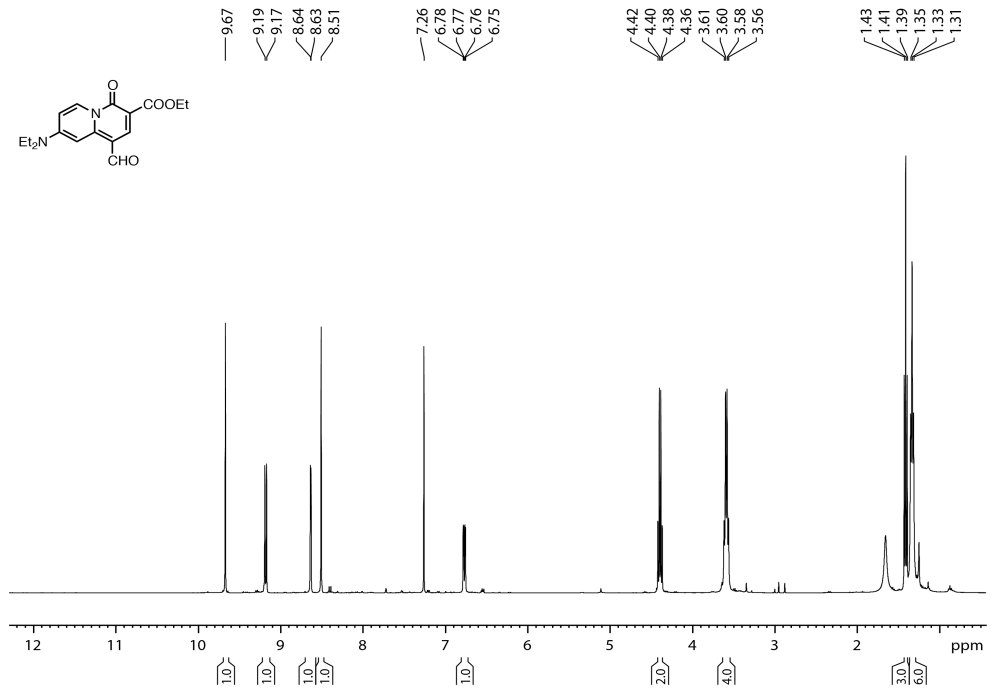

Figure S28. ^{1}H NMR spectrum of **2c** in $CDCl_3$

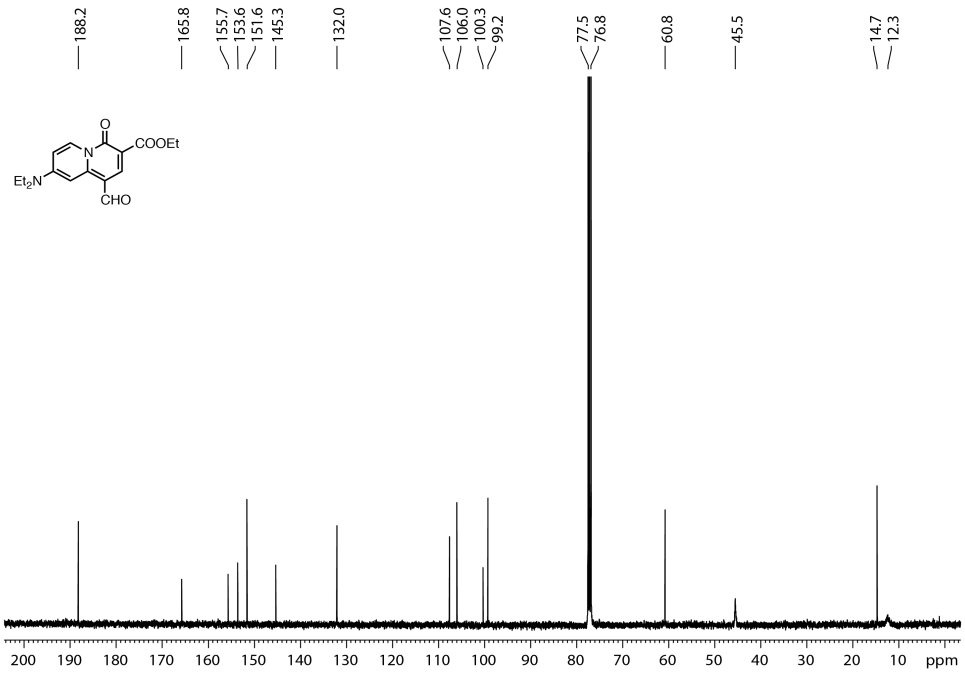

Figure S29. $^{13}C\{^{1}H\}$ NMR spectrum of **2c** in $CDCl_3$

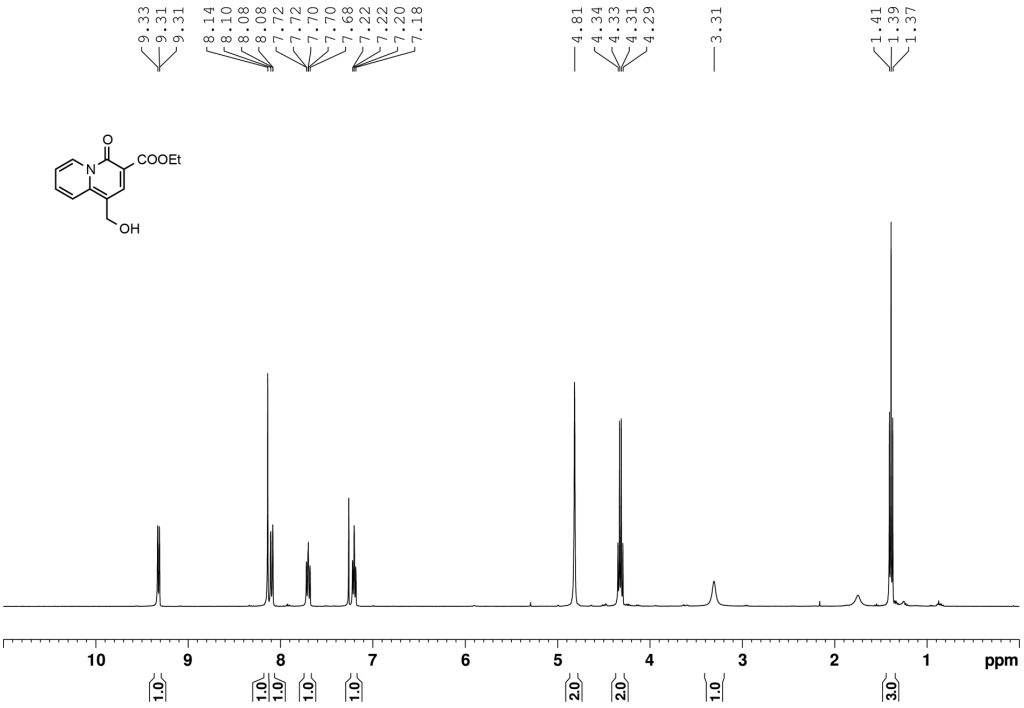

Figure S30. ^{1}H NMR spectrum of **3a** in $CDCl_3$

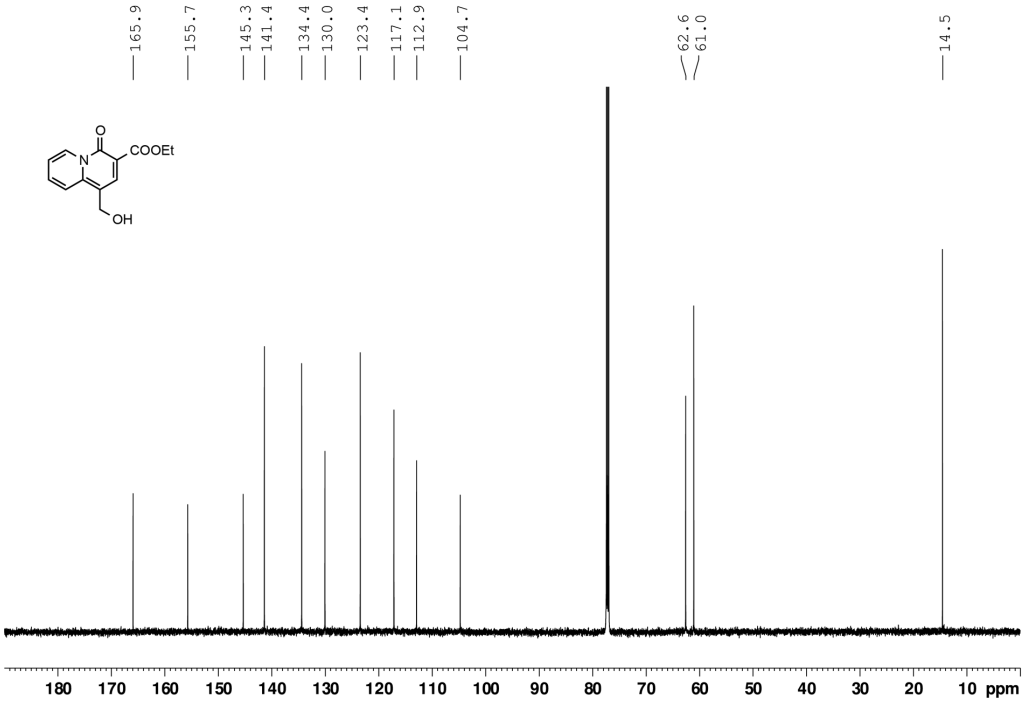

Figure S31. $^{13}C\{^{1}H\}$ NMR spectrum of **3a** in $CDCl_3$

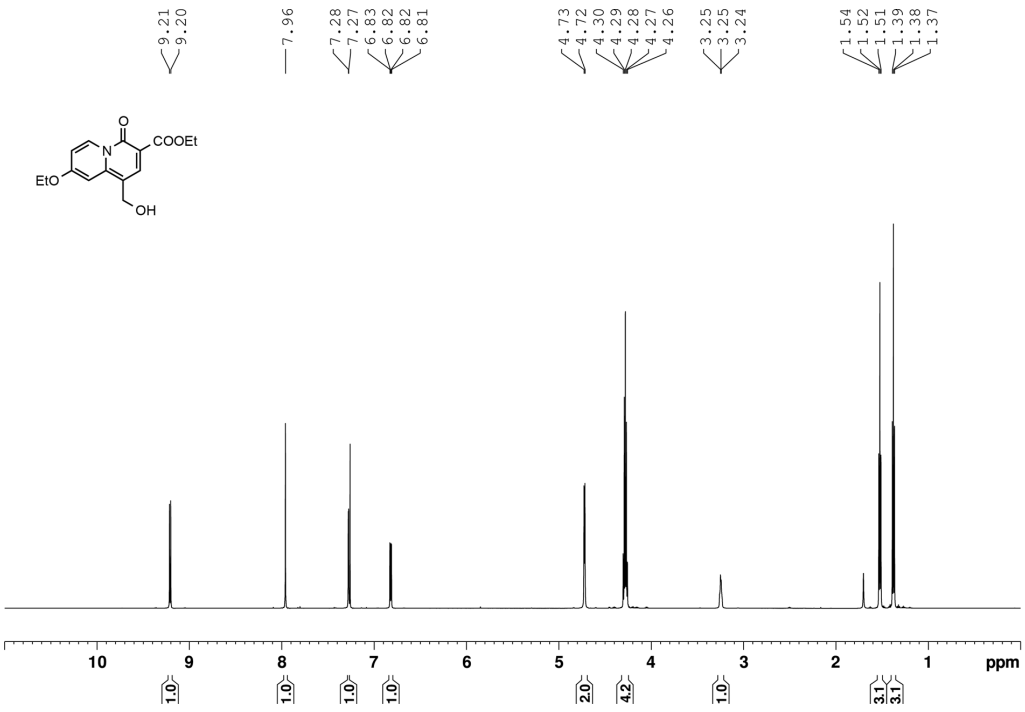

Figure S32. ^{1}H NMR spectrum of **3b** in $CDCl_3$

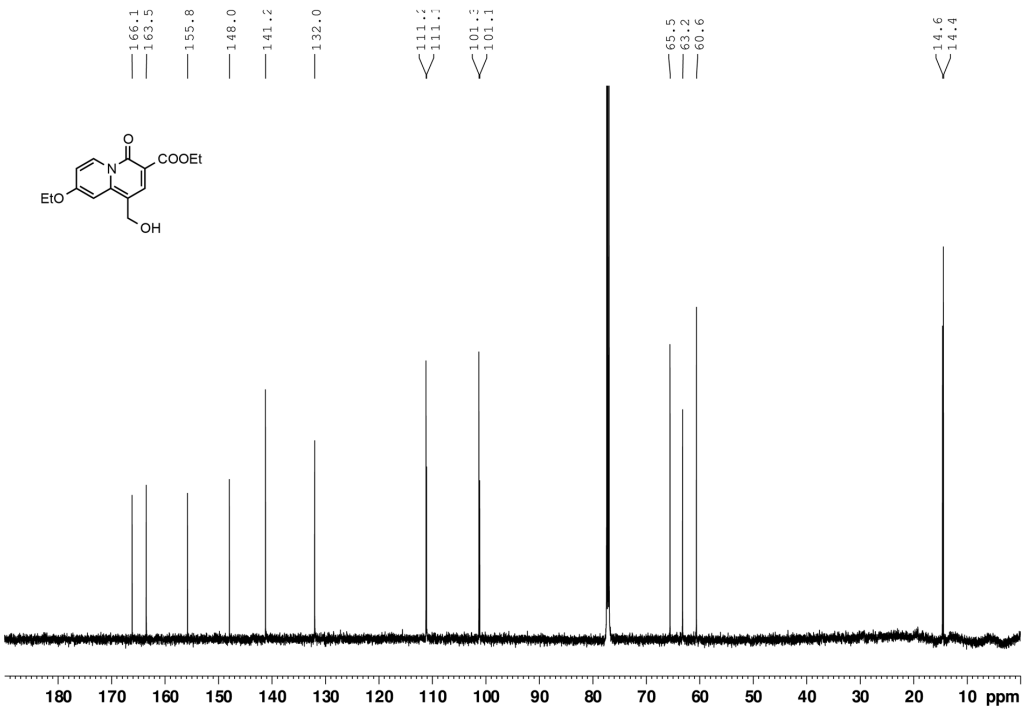

Figure S33. $^{13}C\{^{1}H\}$ NMR spectrum of **3b** in $CDCl_3$

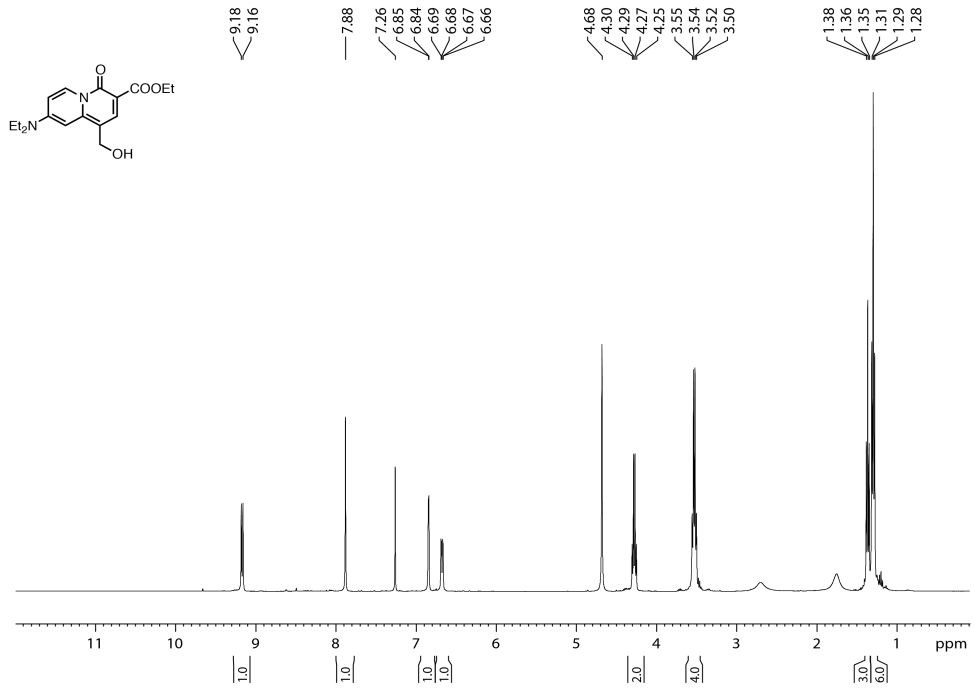

Figure S34. ^{1}H NMR spectrum of **3c** in $CDCl_3$

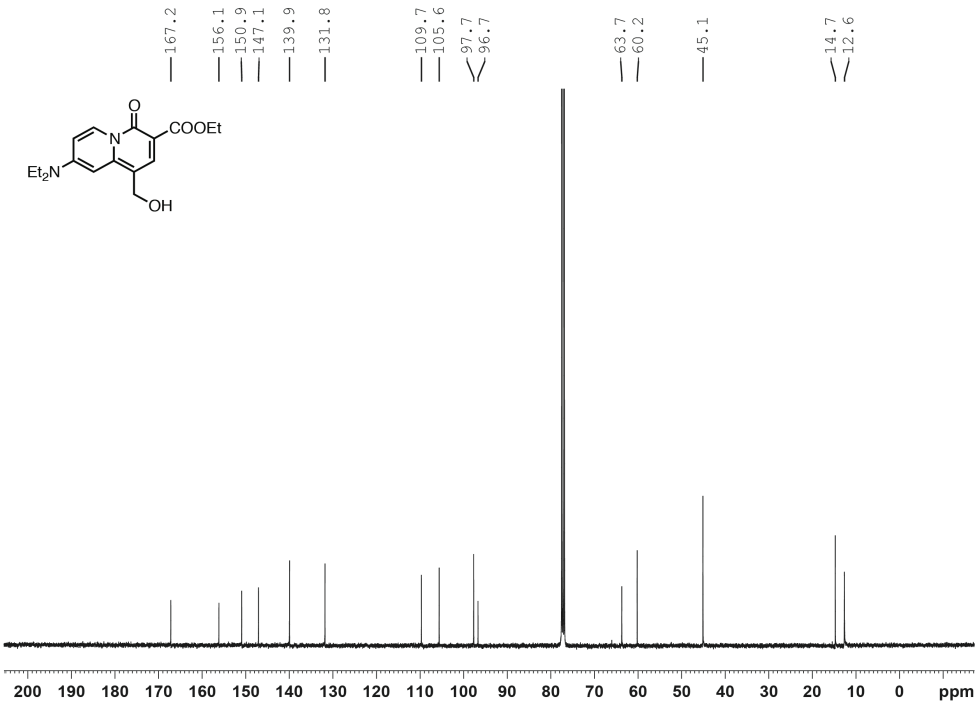

Figure S35. $^{13}C\{^{1}H\}$ NMR spectrum of **3c** in $CDCl_3$

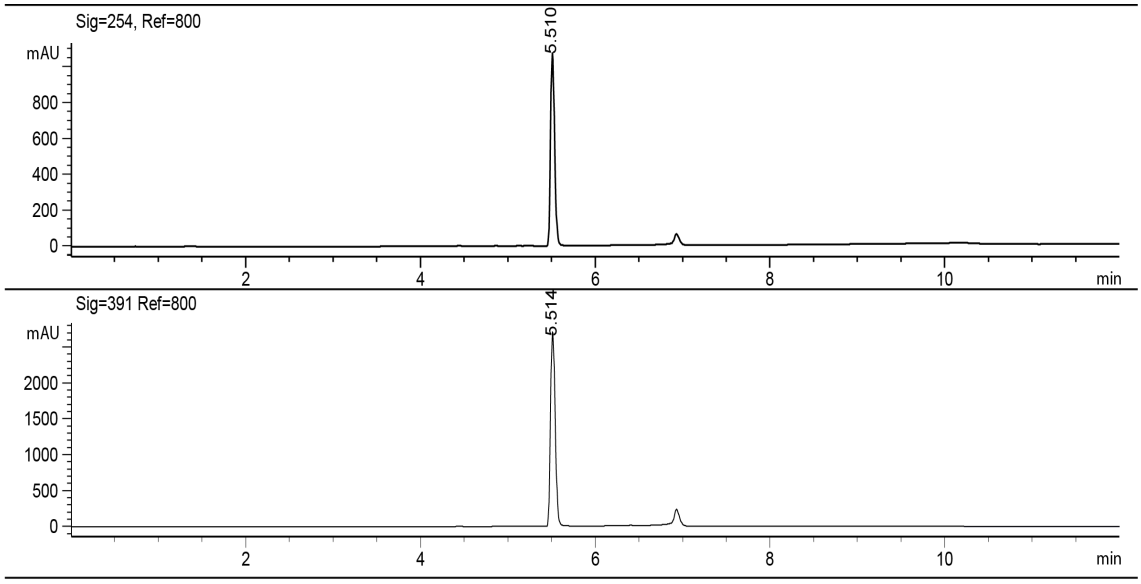

Figure S36. Reversed phase HPLC chromatogram of **3c**, eluted with 10% to 100% acetonitrile/ water (+0.1% TFA) gradient.

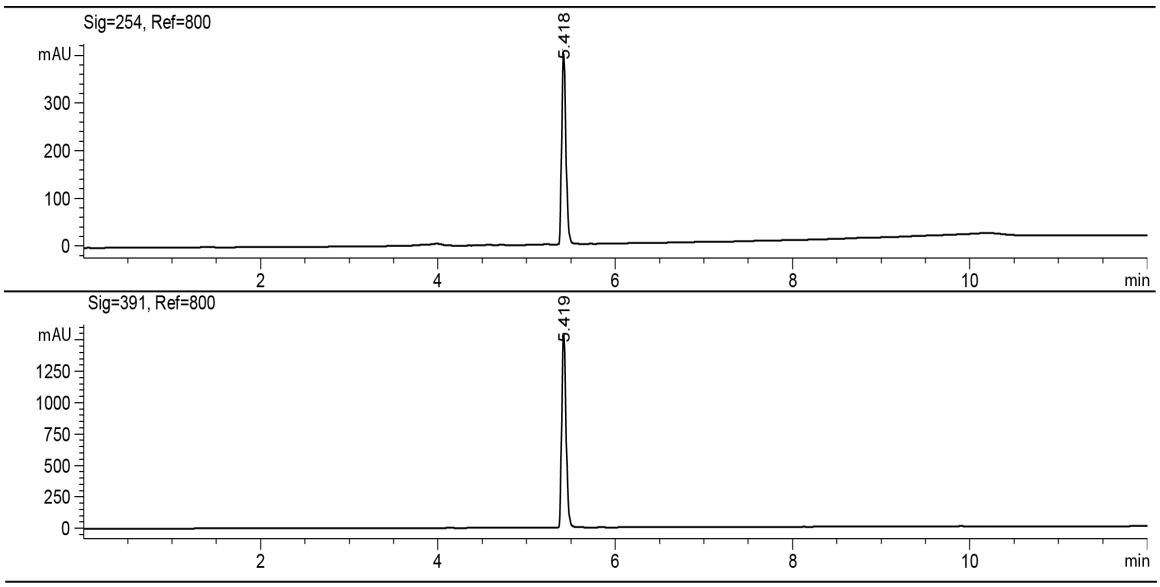

Figure S37. Reversed phase HPLC chromatogram of **7c**, eluted with 10% to 100% acetonitrile/ water (+0.1% TFA) gradient.

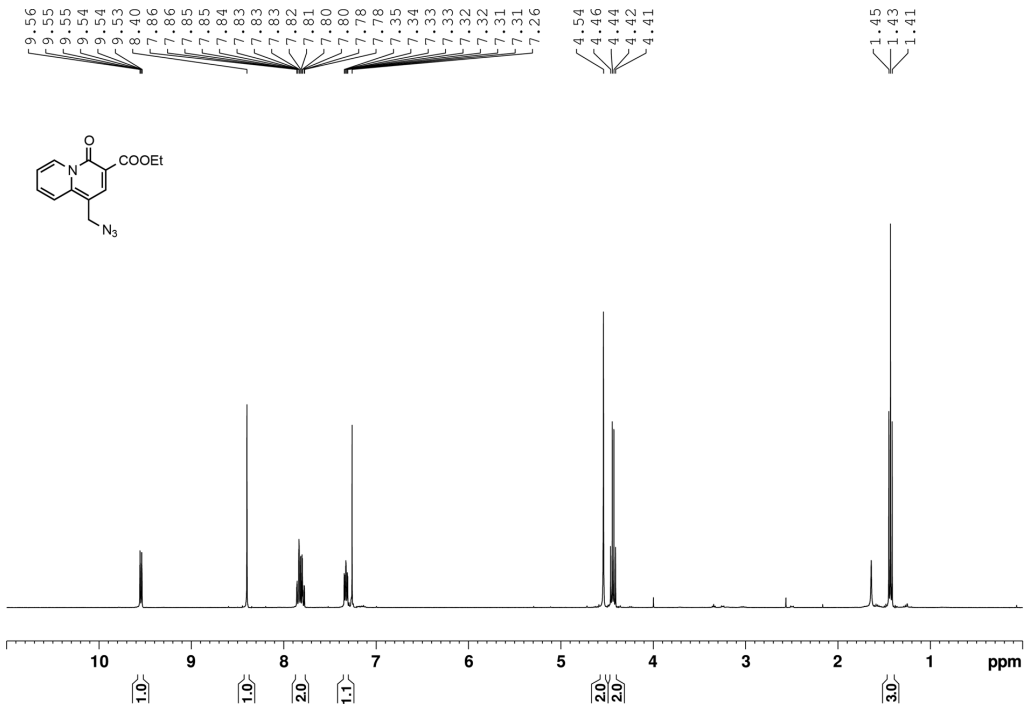

Figure S38. ^{1}H NMR spectrum of **4a** in $CDCl_3$

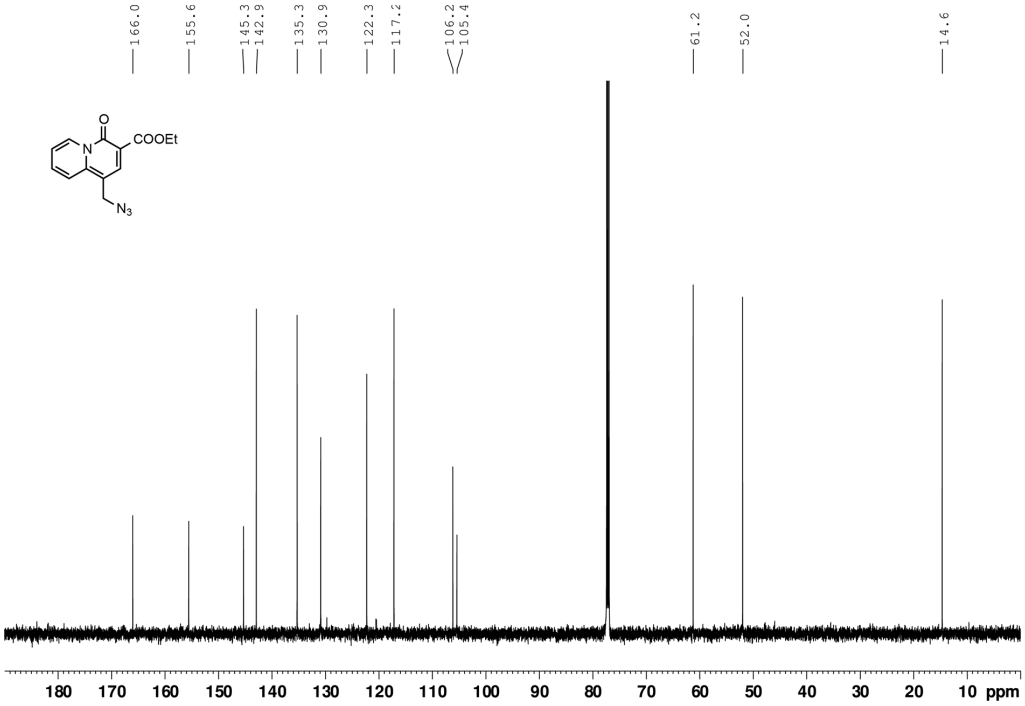

Figure S39. $^{13}C\{^{1}H\}$ NMR spectrum of **4a** in $CDCl_3$

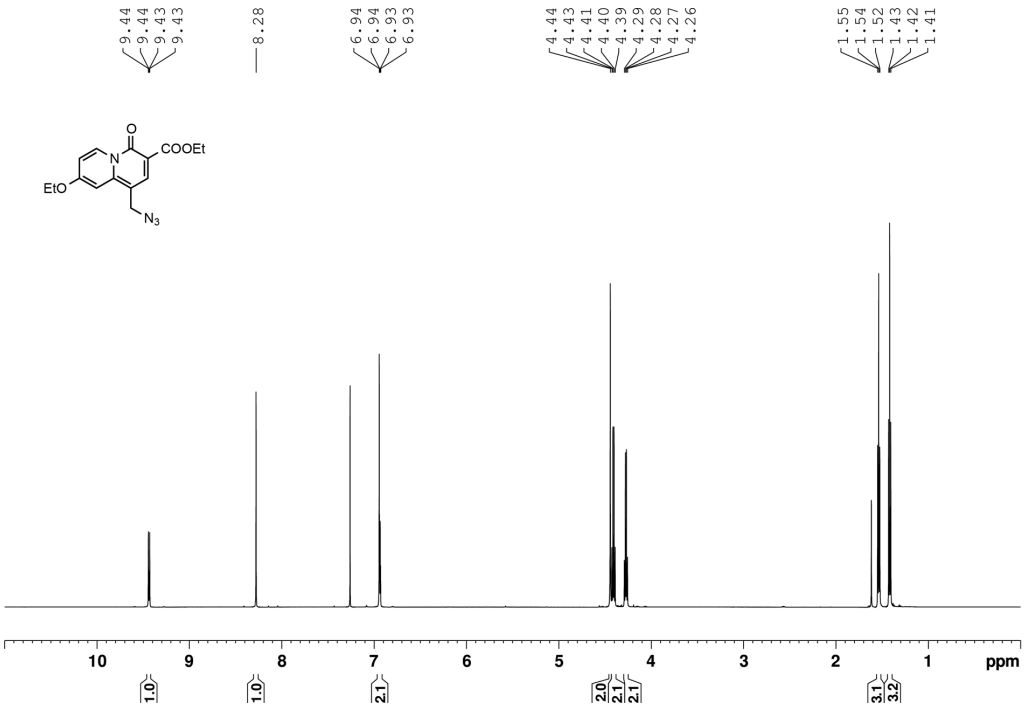

Figure S40. ^{1}H NMR spectrum of **4b** in $CDCl_3$

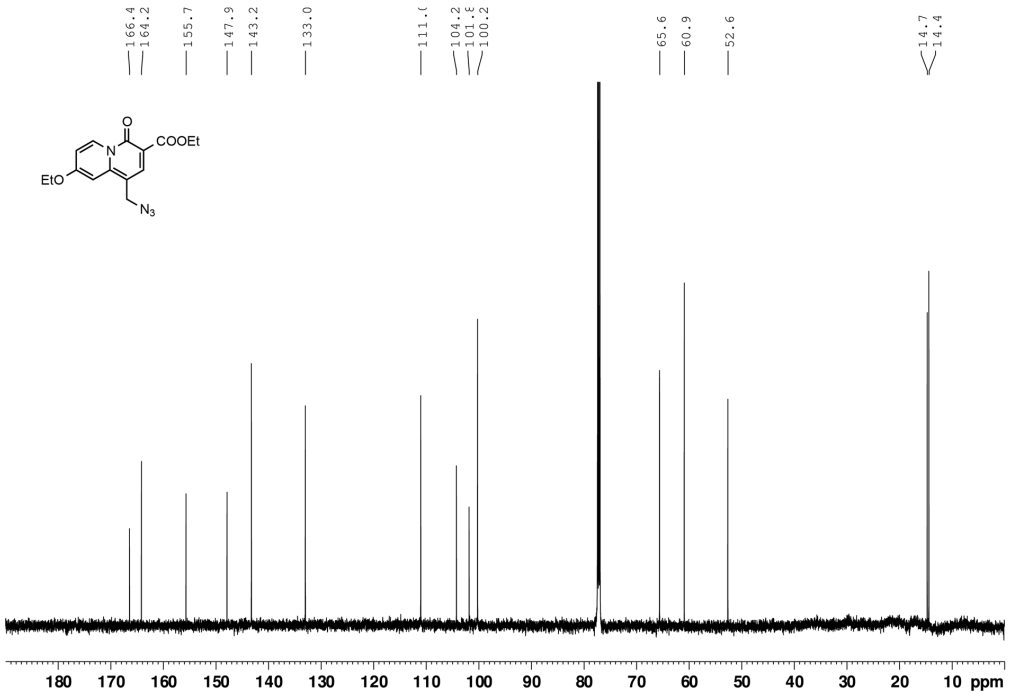

Figure S41. $^{13}C\{^{1}H\}$ NMR spectrum of **4b** in $CDCl_3$

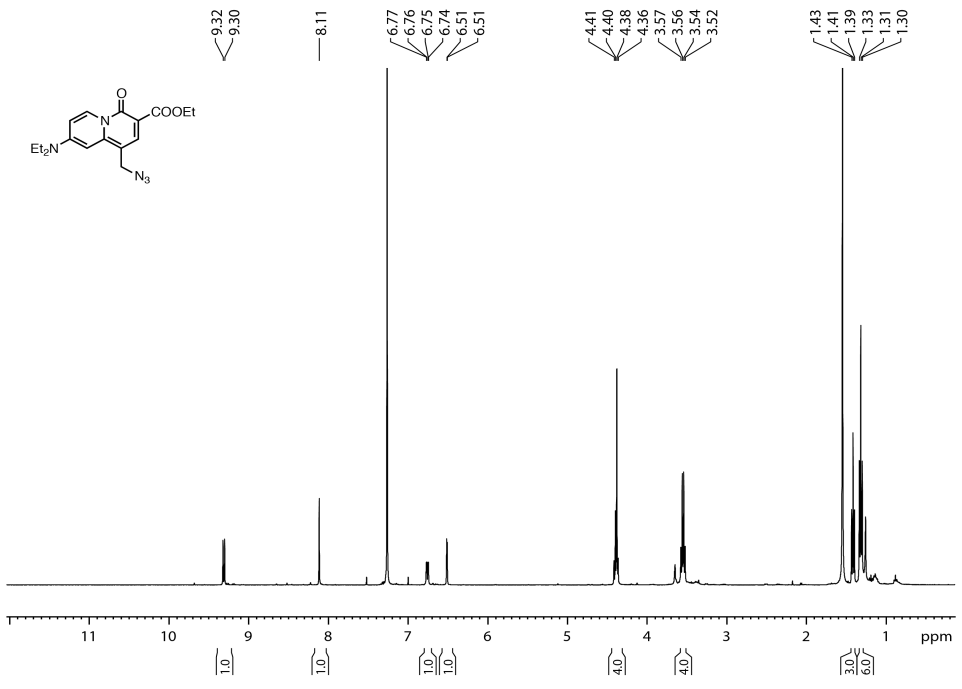

Figure S42. ^{1}H NMR spectrum of **4c** in $CDCl_3$

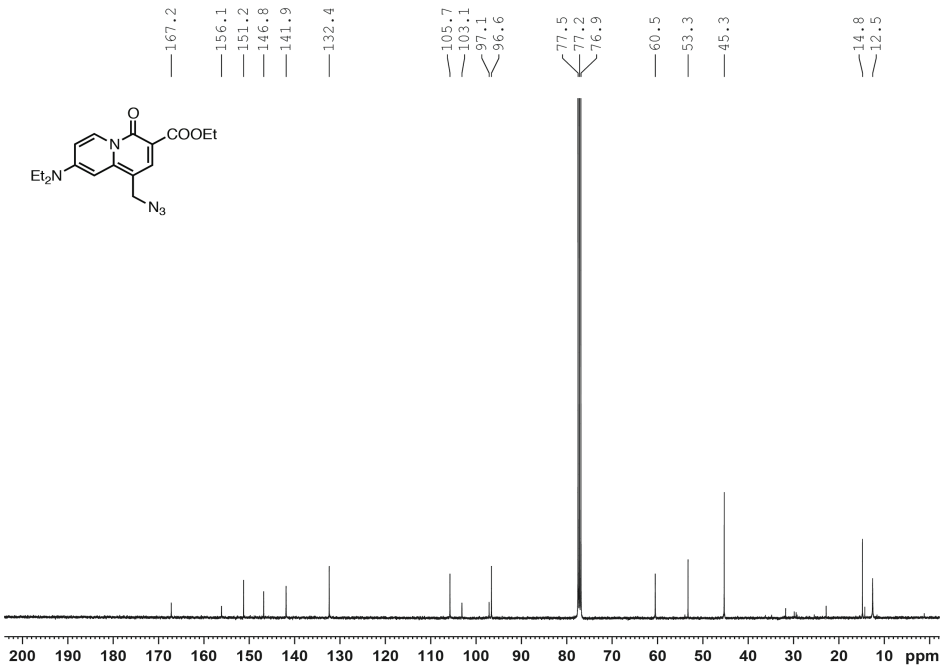

Figure S43. $^{13}C\{^{1}H\}$ NMR spectrum of **4c** in $CDCl_3$

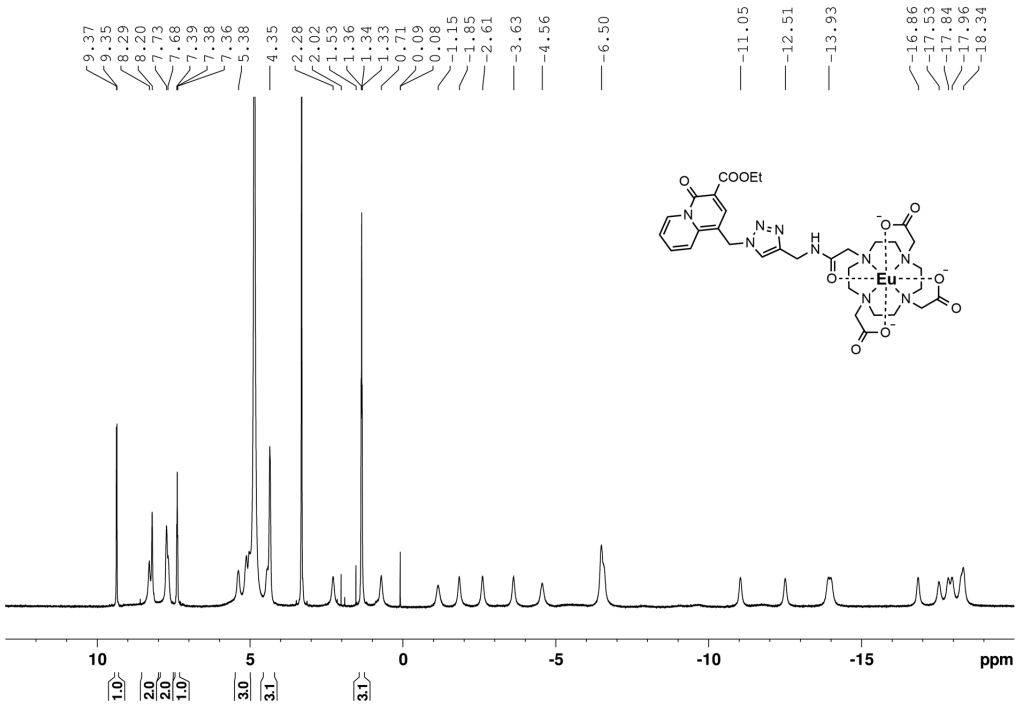

Figure S44. ^{1}H NMR spectrum of **5a** in CD_3OD

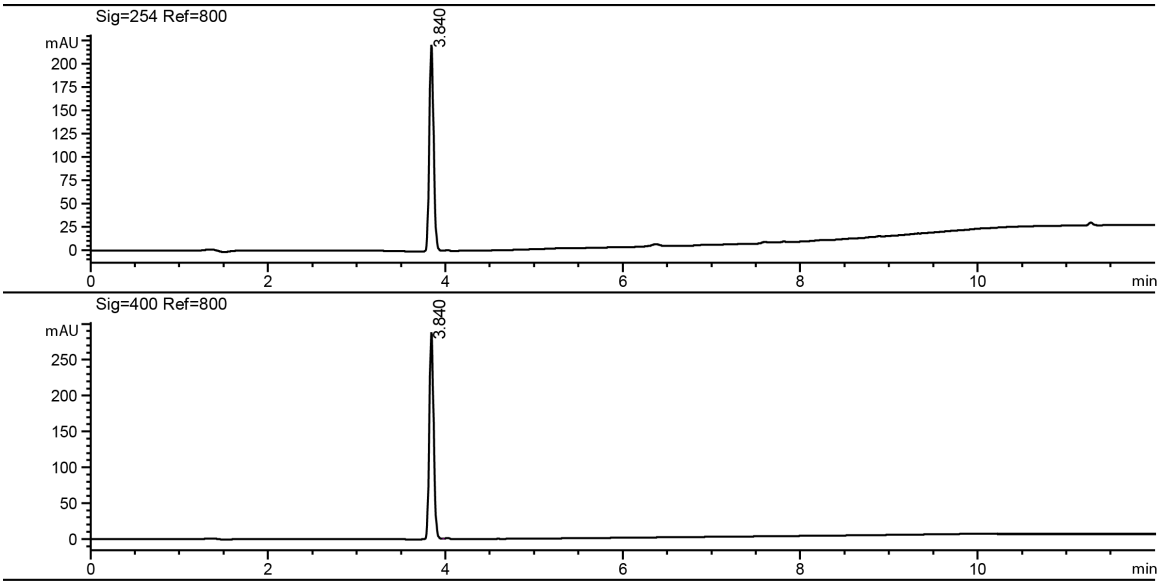

Figure S45. Reversed phase HPLC chromatogram of **5a**, eluted with 10% to 100% acetonitrile/ water (+0.1% TFA) gradient.

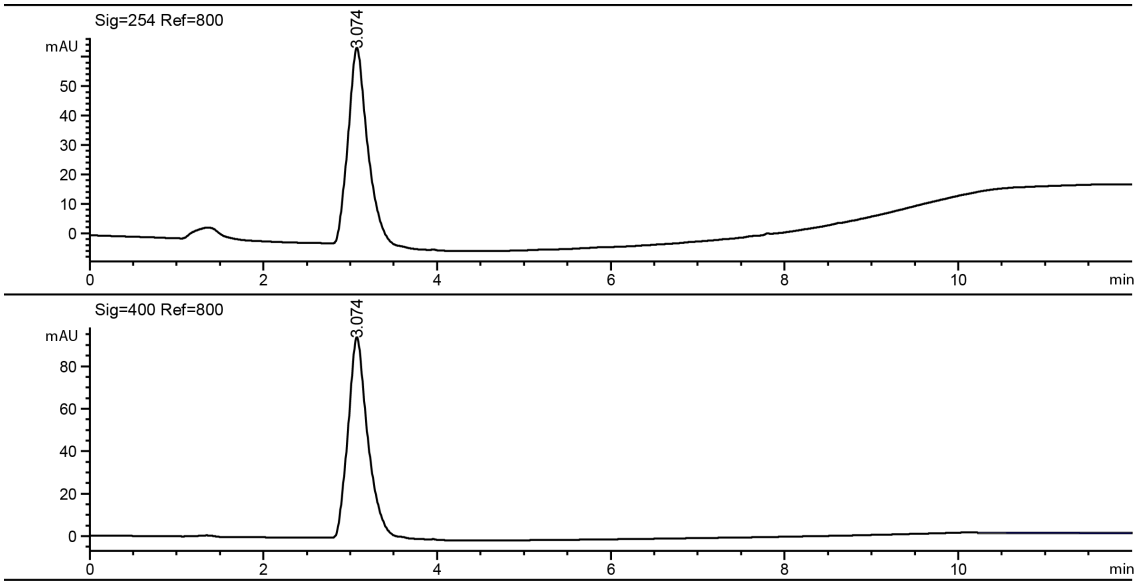

Figure S46. Reversed phase HPLC chromatogram of **MagQEu1**, eluted with 10% to 100% acetonitrile/ water (+0.1% TFA) gradient.

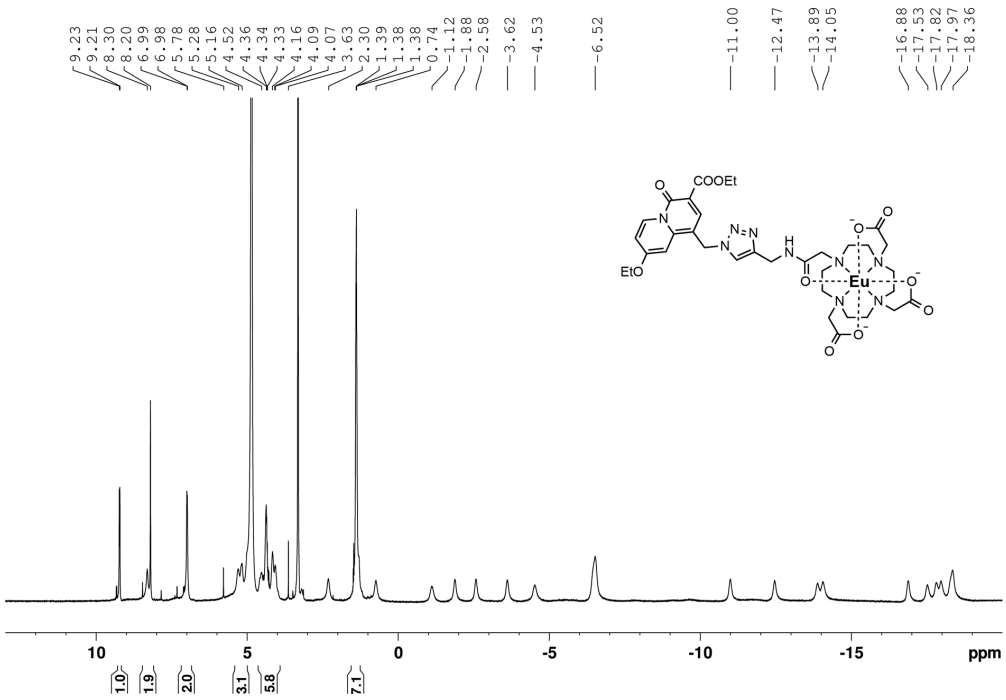

Figure S47. ^{1}H NMR spectrum of **5b** in CD_3OD

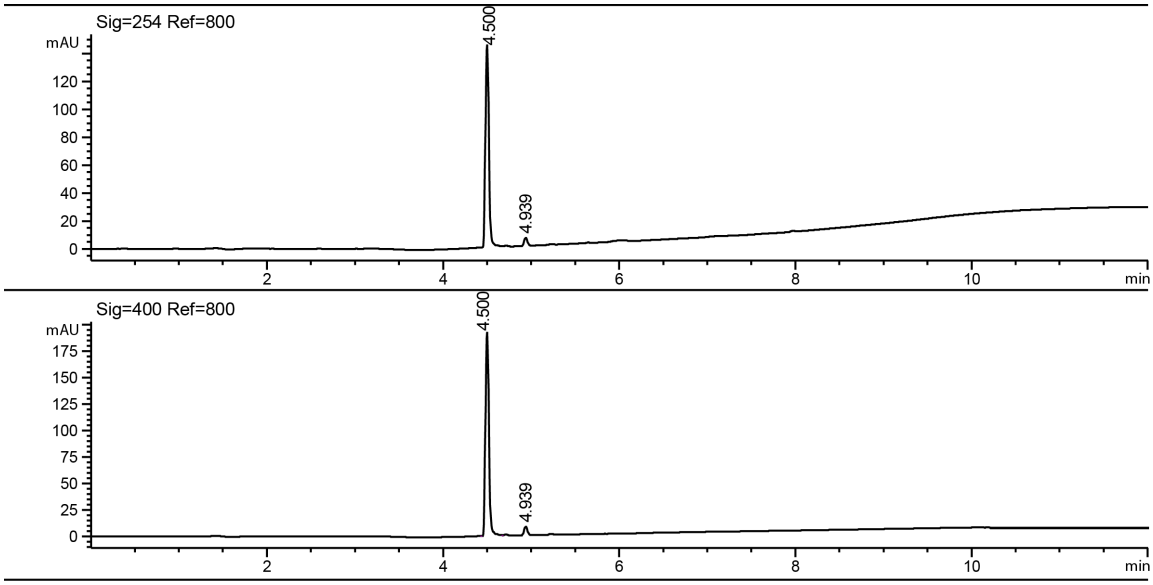

Figure S48. Reversed phase HPLC chromatogram of **5b**, eluted with 10% to 100% acetonitrile/ water (+0.1% TFA) gradient.

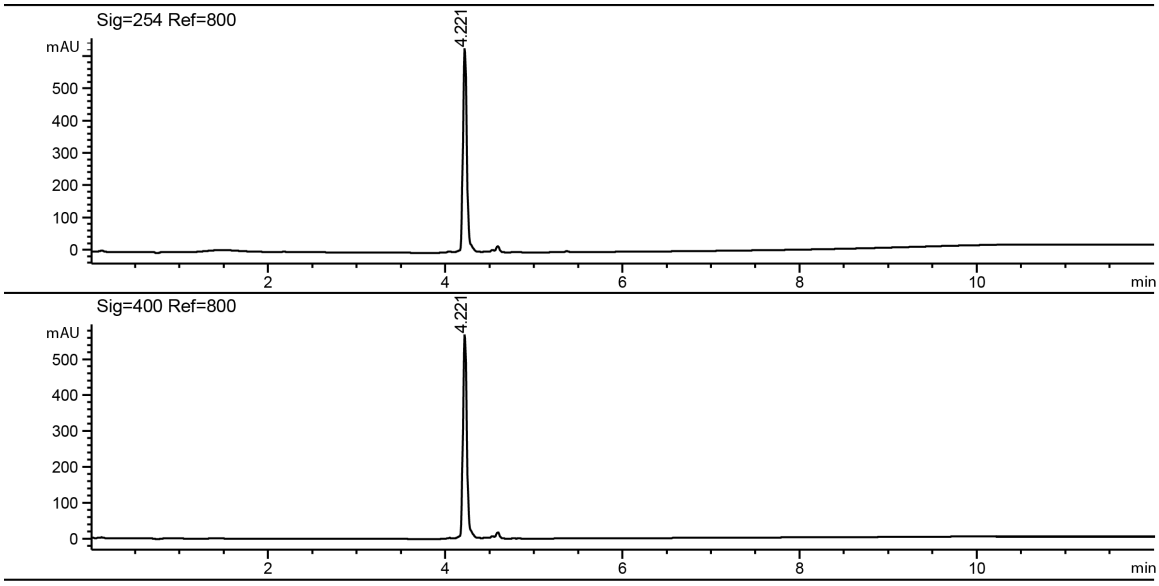

Figure S49. Reversed phase HPLC chromatogram of **MagQEu2**, eluted with 10% to 100% acetonitrile/ water (+0.1% TFA) gradient.

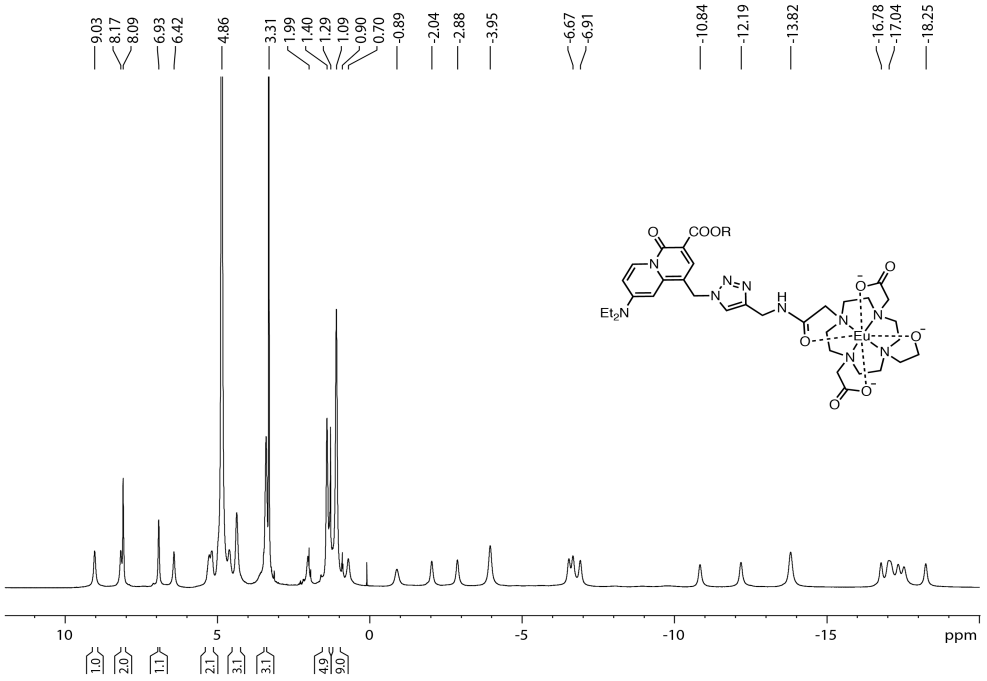

Figure S50. ^{1}H NMR spectrum of **5c** in CD_3OD

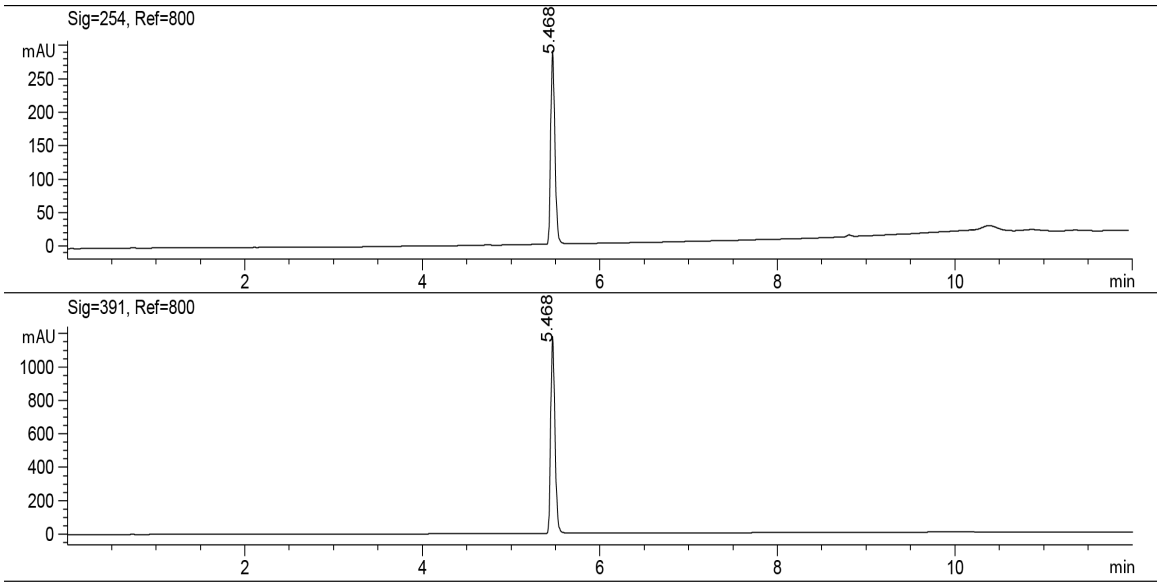

Figure S51. Reversed phase HPLC chromatogram of **5c**, eluted with 10% to 100% acetonitrile/ water (+0.1% TFA) gradient.

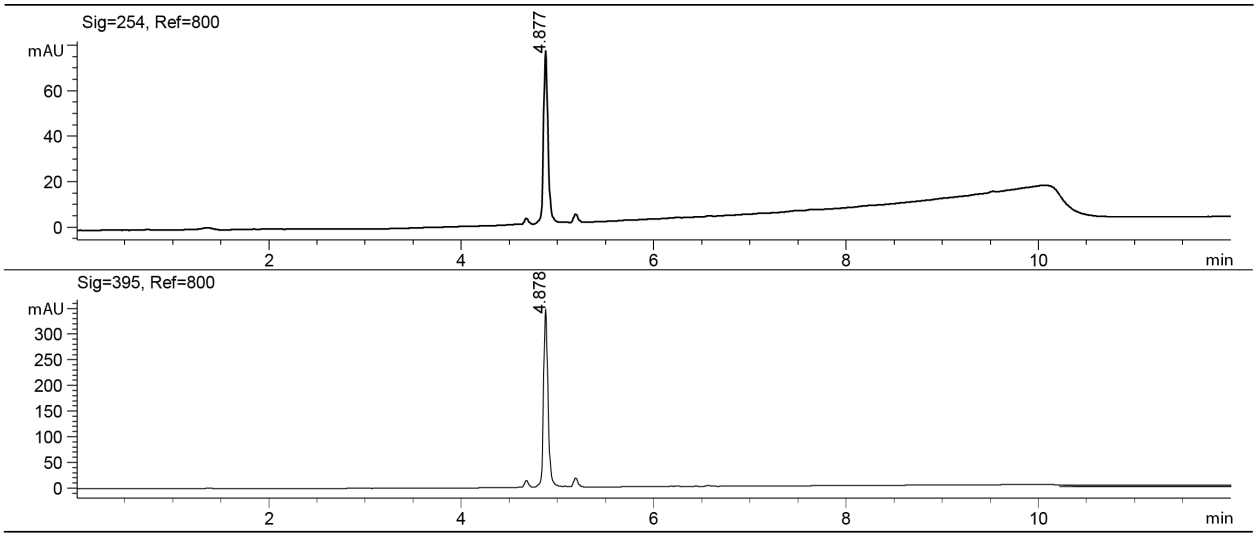

Figure S52. Reversed phase HPLC chromatogram of **MagQEu3**, eluted with 10% to 100% acetonitrile/ water (+0.1% TFA) gradient.

S4. References

1. R. M. Supkowski and W. D. Horrocks, *Inorg. Chim. Acta*, 2002, **340**, 44-48.
2. C. A. M. Seidel, A. Schulz and M. H. M. Sauer, *J. Phys. Chem.*, 1996, **100**, 5541-5553.
3. P. A. Otten, R. E. London and L. A. Levy, *Bioconj. Chem.*, 2001, **12**, 203-212.
4. R. F. H. Viguier and A. N. Hulme, *J. Am. Chem. Soc.*, 2006, **128**, 11370-11371.
5. G. R. Fulmer, A. J. M. Miller, N. H. Sherden, H. E. Gottlieb, A. Nudelman, B. M. Stoltz, J. E. Bercaw and K. I. Goldberg, *Organometallics*, 2010, **29**, 2176-2179.
6. Q. Lin, J. J. Gruskos and D. Buccella, *Org. Biomol. Chem.*, 2016, **14**, 11381-11388.
7. N. G. Connelly and W. E. Geiger, *Chem. Rev.*, 1996, **96**, 877-910.